J. Fluid Mech. (1989), *vol.* 204, *pp.* 185–228
Printed in Great Britain

A canonical statistical theory of oceanic internal waves

By KENNETH R. ALLEN[1] AND RICHARD I. JOSEPH[2]

[1] The Johns Hopkins University, Applied Physics Laboratory, Laurel, MD 20707-6099, USA

[2] Department of Electrical and Computer Engineering, The Johns Hopkins University, Baltimore, MD 21218, USA

(Received 9 June 1988 and in revised form 4 January 1989)

We use the methods of statistical mechanics to develop a theoretical relationship between the observed oceanic spectra and the probability distributions usually studied in statistical mechanics. We also find that the assumption that in terms of Lagrangian variables the oceanic internal wave field is near canonical equilibrium (i.e. the internal wave modes are populated in accordance with a Maxwell–Boltzmann-type distribution) yields expressions for the various marginal or reduced Eulerian spectra associated with both moored and towed measurements which are in striking qualitative agreement with experiment. In developing this theory it is important to distinguish carefully between Lagrangian and Eulerian variables. The important difference between the two sets of variables is due to the advective nonlinearity (i.e. $(\boldsymbol{v}\cdot\nabla)\boldsymbol{v}$ where $\boldsymbol{v}$ is the Eulerian velocity) which is present only in the Eulerian frame. Our method treats the dynamics within the Lagrangian frame, where because of the absence of the advective nonlinearity it is fundamentally simpler, and then transforms to the Eulerian or measurement frame. We find that at small wavenumbers the four-dimensional Eulerian frequency wavenumber spectrum is approximately equal to the corresponding Lagrangian frequency wavenumber spectrum. At large wavenumbers, however, advective contributions become important and the two types of spectra are significantly different. While from a Lagrangian frame point of view the system is entirely wavelike, at large wavenumbers the Eulerian spectrum is not confined to the dispersion surface and the system, from an Eulerian frame point of view, is not wavelike. Further, the three-dimensional Eulerian wavenumber spectrum exhibits a large-wavenumber advective tail which decays as a power law and results in one-dimensional marginal spectra which are in excellent qualitative agreement with experiment. The above features are exhibited independent of the detailed nature of the underlying Lagrangian frequency wavenumber spectrum.

1. Introduction

In this paper we consider the application of some methods from classical statistical mechanics to the problem of calculating the various fluctuation spectra observed in the ocean. We are concerned here with those lengthscales and timescales which are typically ascribed to internal waves. The model variance spectrum suggested by Garrett & Munk (1972, 1975, hereinafter GM), has synthesized a variety of oceanic temperature and velocity data into a single unifying structure. The *model assumes* that these fields are due to a random superposition of linear internal waves and that the covariance matrix associated with a joint amplitude distribution function is

diagonal in both vertical mode number and horizontal wavevector. The diagonal elements of the covariance matrix are then empirically adjusted to obtain agreement between their model and various marginal or reduced spectra associated with the above observed fields. While the GM model provides a useful and surprisingly reliable catalogue of existing experiments, it is empirical and does not presume to provide a theoretical explanation for the various observed spectra. It is our goal in this paper to develop a clear theoretical relationship between the observed oceanic spectra and the probability distributions which are usually studied in statistical mechanics (Prigogine 1962; Mori 1965; Fox 1978; van Kampen 1976).

In developing this theory it will be important to distinguish carefully between Lagrangian and Eulerian variables. In order to clarify this point we need to examine briefly the important difference between Lagrangian and Eulerian variables. In a Lagrangian formulation the fluid is divided into a number of microscopically large but macroscopically small parcels that are identified by the various values of a three-dimensional parameter which we shall denote by the vector $\boldsymbol{r}$. While it is not necessary, it is usually the case that $\boldsymbol{r}$ corresponds to the position of the parcel under some reference condition often taken to be the undisturbed or static condition. Once selected, a specific value for $\boldsymbol{r}$ remains with the fluid parcel and does not change throughout the dynamic evolution of the system. We shall denote the Lagrangian displacement by $\boldsymbol{s}_{\mathrm{L}}(\boldsymbol{r}, t)$ and the Lagrangian velocity by $\boldsymbol{v}_{\mathrm{L}}(\boldsymbol{r}, t)$ where t is time. The Eulerian displacement will be denoted by $\boldsymbol{s}_{\mathrm{E}}(\boldsymbol{x}, t)$ and the Eulerian velocity by $\boldsymbol{v}_{\mathrm{E}}(\boldsymbol{x}, t)$ where a given value for the Eulerian label $\boldsymbol{x}$ corresponds to a specific point in space and refers to the fluid parcel which happens to be at that point at the time t. Thus, a given value for the Eulerian label $\boldsymbol{x}$ does not always refer to the same fluid parcel. A formulation in terms of Lagrangian variables retains a faithful correspondence with the particles of Newtonian mechanics. Such a formulation can be given in terms of a Hamiltonian and Hamilton's canonical equations, or the Lagrangian variables can be used directly with Hamilton's principle to obtain the well-known variational form of continuum mechanics. It is the distribution of these variables which is usually studied in statistical mechanics. In the case of Eulerian variables no such straightforward Hamiltonian formulation is possible. While the Eulerian equations of motion have been cast into a variational form (e.g. Seliger & Whitham 1968; Henyey 1983) which is sometimes referred to as canonical, such a formulation requires the introduction of additional variables and constraints and is significantly different from the usual well-known Hamiltonian dynamics. The important difference between the Eulerian and Lagrangian equations of motion is the flow term $(\boldsymbol{v}_{\mathrm{E}} \cdot \boldsymbol{\nabla}) \boldsymbol{v}_{\mathrm{E}}$ which occurs in the Eulerian equations but not in the Lagrangian equations.

Most observations and empirical studies of geophysical systems such as the ocean are in terms of Eulerian variables. The GM model, for example, is in terms of Eulerian variables. On the other hand, the methods of statistical mechanics which might be useful for understanding and interpreting these studies are usually formulated in terms of Lagrangian variables. This raises the issue of how to relate statistical quantities, such as spectra, which are given in terms of Lagrangian variables to the corresponding quantities given in terms of Eulerian variables. The difficulty is that in general the exact transformation between the two sets of variables is not tractable. The problem of relating Lagrangian and Eulerian aspects of fluid flow is an old one which goes back at least to G. I. Taylor (1921). For ocean surface waves a recent physical discussion is given by Longuet-Higgins (1986). In a recent paper (Allen & Joseph 1988) it was shown that there exists a class of systems

for which the problem of implementing an exact transformation can be avoided, and still a tractable relation between Lagrangian and Eulerian spectra can be obtained. It was shown that at small wavenumbers the Eulerian and Lagrangian spectra are approximately equal, but at large wavenumbers, independent of the large wavenumber structure of the Lagrangian spectra, the Eulerian wavenumber spectra exhibit a power-law decay. In this paper we will argue that the moored spectra are dominated by small wavenumbers at which the Eulerian and Lagrangian spectra are approximately equal and show that the moored frequency spectra calculated on this basis are in excellent qualitative agreement with experiment. We will further argue that the observed towed spectra are mostly at wavenumbers for which the Eulerian and Lagrangian wavenumber spectra are significantly different, and show that the large-wavenumber power-law decay exhibited by our theoretical Eulerian spectra is in excellent qualitative agreement with experiment. It will also be clear that experiments which focus upon this decaying Eulerian tail cannot yield information about fundamental dynamical processes.

The following is a brief outline of what is done in this paper. We first develop the four-dimensional Lagrangian frequency wavenumber displacement spectra which are proportional to the distribution of energy in frequency ω and three-dimensional wave vector $\boldsymbol{k}$, and discuss the relation between this and the distribution of energy among the linear internal wave modes. We next define the Eulerian variables in terms of the Lagrangian variables and obtain the four-dimensional Eulerian-frequency wavenumber displacement spectrum. It will be clear that in general the two types of spectra are significantly different. Finally, we discuss our results and present a comparison to experiment for a variety of marginal Eulerian spectra and make some suggestions for future investigations. Since the course of this treatment is lengthy and at places a bit tortuous, we devote the rest of this introductory section to a more detailed outline of the important mathematical steps and physical assumptions which can serve as a guide to the development in the following sections.

In our canonical formulation the Cartesian components of the Lagrangian displacement $s_{\mathrm{L}\alpha}(\boldsymbol{r},t)$ and velocity $v_{\mathrm{L}\alpha}(\boldsymbol{r},t), 1 \leqslant \alpha \leqslant 3$, are expressed in the form

$$s_{\mathrm{L}\alpha}(\boldsymbol{r},t) = \sum_{j=1}^{M} \phi_{j\alpha}(\boldsymbol{r})\, q_j(t), \tag{1.1}$$

and

$$v_{\mathrm{L}\alpha}(\boldsymbol{r},t) = \sum_{j=1}^{M} \phi_{j\alpha}(\boldsymbol{r})\, \Omega_j\, p_j(t), \tag{1.2}$$

where the $q_j(t)$ are real independent generalized displacements (a complex representation can also be used), the $p_j(t)$ are the corresponding canonically conjugate momenta, and M is the number of degrees of freedom (later, M will be allowed to become arbitrarily large). In (1.1) and (1.2) the $\phi_{j\alpha}(\boldsymbol{r})$ are real eigenfunctions associated with writing the quadratic part of the Hamiltonian in separated form such that

$$H(p,q) = H_0(p,q) + V_{\mathrm{I}}(p,q) = \sum_{j=1}^{M} (\tfrac{1}{2}\Omega_j)[p_j^2(t) + q_j^2(t)] + V_{\mathrm{I}}(p,q), \tag{1.3}$$

and the Ω_j are the eigenfrequencies associated with the linear internal waves. In (1.3) the term $H_0(p,q)$, which is quadratic in the dynamical variables, corresponds to the linear solutions and we shall refer to it as the free-field Hamiltonian. The term $V_{\mathrm{I}}(p,q)$, which is of cubic and higher order in the dynamical variables, describes the nonlinear interactions and we shall refer to it as the interaction potential. Here

(p, q) denotes the set $\{p_1, q_1, \ldots, p_M, q_M\}$ of canonically conjugate dynamical variables. We point out that in the completely general case there are also modes for which the free-field Hamiltonian is not of the harmonic oscillator type given in (1.3). For example, the translational modes (sometimes called geostrophic or vortical modes) are of the free-particle type which require

$$\bar{H}_0(p, q) = \sum_{j=1}^{M} C_j \bar{p}_j^2(t), \tag{1.4}$$

where the C_j are constants. It is clear that the formulation can be generalized to include such details, but to do so now would increase the already considerable mathematical complexity and tend to obscure the underlying physics. This approximation ignores some potentially important issues concerning the diffusion of fluid parcels, but is adequate for our purposes here.

The Cartesian components of the Eulerian displacement $s_{E\alpha}(\boldsymbol{x}, t)$ and velocity $v_{E\alpha}(\boldsymbol{x}, t)$ can similarly be written in the form

$$s_{E\alpha}(\boldsymbol{x}, t) = \sum_{j=1}^{M} \phi_{j\alpha}(\boldsymbol{x})\, a_j(t), \tag{1.5}$$

and

$$v_{E\alpha}(\boldsymbol{x}, t) = \sum_{j=1}^{M} \phi_{j\alpha}(\boldsymbol{x})\, \Omega_j\, b_j(t). \tag{1.6}$$

While the form of (1.5) and (1.6) is identical to that of (1.1) and (1.2) respectively, in general the $a_j(t)$ and $b_j(t)$ are not related in any simple way to the $q_j(t)$ and $p_j(t)$. The linearized equations of motion for the two sets of variables are the same, so that for small enough amplitude disturbances we may write

$$a_j(t) = q_j(t), \tag{1.7}$$

and

$$b_j(t) = p_j(t). \tag{1.8}$$

However, the nonlinear terms associated with the two sets of variables are different. The dynamic nonlinearities also contribute to the Eulerian equations of motion, but, as previously noted, because individual fluid parcels are constantly flowing into and out of the region of interest there is an additional nonlinear flow term given by $(\boldsymbol{v}_E \cdot \nabla)\, \boldsymbol{v}_E$ which we shall call the advective nonlinearity. Thus, for larger-amplitude disturbances (1.7) and (1.8) are not valid and the exact transformation between the variables becomes intractable. It is important to realize that the two types of nonlinearities are fundamentally different. The dynamic nonlinearities are associated with the details of the forces between collections of fluid parcels. The advective nonlinearity is associated with the flow of fluid parcels into and out of a fixed region of space and is strictly an Eulerian frame concept. From a Lagrangian frame point of view the advective nonlinearity is a kinematic effect. It is, however, important to account for this effect when making comparisons between theory and experiment.

In statistical mechanics it is the distribution of the canonically conjugate variables $p_j(t)$ and $q_j(t)$ which is usually studied. There exists a considerable theoretical precedent to assume that the statistical distribution of the canonically conjugate dynamical variables is of the Gaussian form

$$g(p, q) = \frac{1}{Z} \exp\left\{ - \sum_{j=1}^{M} [p_j^2(t) + q_j^2(t)]/2A_{Lj} \right\}, \tag{1.9}$$

where $g(p, q)$ is the phase-space density function, Z is the partition function (i.e.

normalization factor), and A_{Lj} is the average Lagrangian wave action associated with the jth mode. In general the average wave action is given by

$$A_{Lj} = \frac{\mathcal{A}_j}{\Omega_j}, \tag{1.10}$$

where $\mathcal{A}_j$ is the average energy of the jth mode. The most familiar example of this is canonical equilibrium in the weak interaction approximation (cf. Prigogine 1962) in which the linear energy is equipartitioned among the accessible modes so that the average energy per mode is given by $\mathcal{A}_j = E_0$ which, for the canonical distribution, is independent of the mode index j. The distribution given by (1.9) is more general than the canonical distribution and can include cases for which the wave system is interacting with a generalized heat bath (e.g. source and sink contributions) as well as some cases for which nonlinear interactions from $V_I(p, q)$ are important over at least a part of mode and wavenumber space. We shall give a more detailed discussion of these various cases later, but for now we will simply assume the phase-space density function (1.9) for the general case in which the average wave action is given by (1.10). We defer this discussion until the next section in order not to distract from the direct outline of precisely what is done in this paper.

Once the phase-space density function has been specified, the expectation value $E[F(p, q, t)]$ of any function $F(p, q, t)$ of the Lagrangian dynamical variables is obtained by computing

$$E[F(p,q,t)] = \int F(p,q,t)\, g(p,q) \prod_{j=1}^{M} \mathrm{d}p_j\, \mathrm{d}q_j, \tag{1.11}$$

where unless otherwise noted all integrals in this paper are over the full range of the integration variable. In particular we shall be concerned with the two space point two time point Lagrangian displacement correlation functions $C_{Ls\alpha\beta}(\boldsymbol{r}, \boldsymbol{R}, \tau)$ defined by

$$C_{Ls\alpha\beta}(\boldsymbol{r}, \boldsymbol{R}, \tau) = E[s_{L\alpha}(\boldsymbol{r}+\tfrac{1}{2}\boldsymbol{R}, t+\tau)\, s_{L\beta}(\boldsymbol{r}-\tfrac{1}{2}\boldsymbol{R}, t)], \tag{1.12}$$

where $\boldsymbol{r}$ is midway between the two space points separated by $\boldsymbol{R}$ and we have anticipated temporal stationarity (i.e. the correlation functions are independent of the reference time t). The four-dimensional Lagrangian frequency wavenumber spectra $S_{Ls\alpha\beta}(\boldsymbol{r}, \boldsymbol{k}, \omega)$ are then defined as

$$S_{Ls\alpha\beta}(\boldsymbol{r}, \boldsymbol{k}, \omega) = \int \mathrm{d}^3R \int \mathrm{d}\tau\, C_{Ls\alpha\beta}(\boldsymbol{r}, \boldsymbol{R}, \tau) \exp\{-\mathrm{i}(\boldsymbol{k}\cdot\boldsymbol{R} - \omega\tau)\}. \tag{1.13}$$

We note that in the usual oceanic case the system is horizontally homogeneous (i.e. independent of the horizontal components of $\boldsymbol{r}$) but because of vertical stratification and the free-surface boundary condition these spectra generally depend upon the depth. The four-dimensional Lagrangian frequency wavenumber spectra and their Eulerian counterparts (to be defined shortly) provide the basis in terms of which the studies in this paper are conducted.

The correlation functions given by (1.12) involve the two times t and $t+\tau$. In order to use (1.11) to calculate the expectation value we must express the displacement at the time $t+\tau$ in terms of the canonically conjugate variables $p_j(t)$ and $q_j(t)$ and explicit functions of τ. For this purpose we will use

$$p_j(t+\tau) = p_j(t)\cos(\Omega_j\tau) - q_j(t)\sin(\Omega_j\tau), \tag{1.14}$$

and

$$q_j(t+\tau) = q_j(t)\cos(\Omega_j\tau) + p_j(t)\sin(\Omega_j\tau), \tag{1.15}$$

which correspond to the linear approximation, but can also be used to approximate the short-time dependence in the weak interaction approximation. In a full treatment of the weak interaction approximation the various correlation functions exhibit a slow exponential decay with time. If this decay rate is small in comparison to the corresponding frequency, then the approximation given by (1.14) and (1.15) is valid. We can then use (1.1) and (1.9)–(1.15) to compute the various Lagrangian displacement correlation functions and the corresponding frequency wavenumber spectra. These results will be given in terms of the average Lagrangian wave action $A_{\mathrm{L}j}$ which through (1.10) is a measure of the distribution of energy among the linear internal wave modes. This energy distribution (i.e. A_j) must ultimately be specified, and we shall consider several important cases later, but our primary purpose is to establish a clear theoretical relationship between the observed Eulerian spectra and the fundamental Lagrangian energy distribution.

Our discussion to this point has focused primarily upon the calculation of the Lagrangian correlation functions and spectra. We shall now turn our attention to the calculation of the corresponding Eulerian quantities. The GM result can be obtained by assuming that the Eulerian amplitudes $a_j(t)$ and $b_j(t)$ are distributed in accordance with the Gaussian form (1.9) with $A_{\mathrm{L}j}$ replaced by the average Eulerian wave action $A_{\mathrm{E}j}$ and the replacements indicated by (1.7) and (1.8). It is the Eulerian wave action $A_{\mathrm{E}j}$ which is empirically adjusted by GM to obtain agreement with the observed spectra. While this procedure provides an empirical description of the observed spectra, it does not provide the link between the observed spectra and the fundamental distributions which are studied in statistical mechanics. In order to obtain this link we define the Eulerian displacement in terms of the Lagrangian displacement by the relation

$$s_{\mathrm{E}\alpha}(\boldsymbol{x},t) = \int \mathrm{d}^3 r\, s_{\mathrm{L}\alpha}(\boldsymbol{r},t)\,\delta(\boldsymbol{x}-\boldsymbol{y})\,J(\boldsymbol{s}), \tag{1.16}$$

where $\delta(\boldsymbol{x}-\boldsymbol{y})$ is a three-dimensional delta function,

$$\boldsymbol{y} = \boldsymbol{r}+\boldsymbol{s}(\boldsymbol{r},t), \tag{1.17}$$

and $J(\boldsymbol{s})$ is the Jacobian determinant associated with the transformation (1.17). Equation (1.16) is a well-known relation (Green 1954; Mori, Oppenheim & Ross 1962; Hardy 1963) which can be used to express any Eulerian variable (e.g. $v_{\mathrm{E}\alpha}(\boldsymbol{x},t)$) in terms of the corresponding Lagrangian quantity. It has recently been used by Abarbanel & Rouhi (1987) in a hydrodynamic context to express the Eulerian mass density in terms of Lagrangian variables.

The two space point two time point Eulerian displacement correlation functions $C_{\mathrm{Es}\alpha\beta}(\boldsymbol{x},\boldsymbol{X},\tau)$ are defined by

$$C_{\mathrm{Es}\alpha\beta}(\boldsymbol{x},\boldsymbol{X},\tau) = E[s_{\mathrm{E}\alpha}(\boldsymbol{x}+\tfrac{1}{2}\boldsymbol{X},t+\tau)\,s_{\mathrm{E}\beta}(\boldsymbol{x}-\tfrac{1}{2}\boldsymbol{X},t)], \tag{1.18}$$

where $\boldsymbol{X}$ is the separation between the two space points. The corresponding four-dimensional frequency wavenumber spectra are defined by

$$S_{\mathrm{Es}\alpha\beta}(\boldsymbol{x},\boldsymbol{k},\omega) = \int \mathrm{d}^3 X \int \mathrm{d}\tau\, C_{\mathrm{Es}\alpha\beta}(\boldsymbol{x},\boldsymbol{X},\tau)\exp\{-\mathrm{i}(\boldsymbol{k}\cdot\boldsymbol{X}-\omega\tau)\}. \tag{1.19}$$

We note that since $J(\boldsymbol{s})\,\mathrm{d}^3 r = \mathrm{d}^3 y$, (1.16) obviously yields the usual relation between Lagrangian and Eulerian displacements. However, in order to implement that relation we must invert (1.17) with $\boldsymbol{y} = \boldsymbol{x}$ to find $\boldsymbol{r}$ as a function of $\boldsymbol{x}$ and t. In all but the most simple cases the inversion of (1.17) is intractable and, hence, (1.16) is not useful as an exact point relation between Lagrangian and Eulerian fields. On the

other hand, if (1.16) is used in (1.18) and the phase-space density function given by (1.9) is used to compute the expectation value, then the need to invert (1.17) does not arise and tedious but entirely tractable calculations result. By using this procedure we can obtain expressions for the Eulerian correlation functions and spectra in terms of the Lagrangian spectra.

In §2 we obtain expressions for the four-dimensional Lagrangian frequency wavenumber spectrum. In order to explore some of the details we consider a simple model for internal waves with a constant Väisälä profile and use periodic boundary conditions in the vertical as well as the horizontal. This results in correlation functions and spectra which are homogeneous in both the vertical and the horizontal directions. As an example, we find that the frequency wavenumber spectrum $S_{\mathrm{Ls}33}(\boldsymbol{k},\omega)$ associated with the vertical displacement ($\alpha = 1,2$ corresponds to the horizontal directions and $\alpha = 3$ corresponds to the vertical direction) is given by

$$S_{\mathrm{Ls}33}(\boldsymbol{k},\omega) = \frac{\pi k_{\mathrm{h}}^2 \Lambda(\boldsymbol{k})}{\rho k^2 \Omega^2(\boldsymbol{k})}[\delta(\Omega(\boldsymbol{k})-\omega)+\delta(\Omega(\boldsymbol{k})+\omega)], \tag{1.20}$$

where, because the system is homogeneous, we have suppressed display of the label $\boldsymbol{r}$. In (1.20) ρ is the fluid density, k_{h} is the magnitude of the horizontal component of $\boldsymbol{k}$, k is the magnitude of $\boldsymbol{k}$, and we have allowed the volume of the ocean to become arbitrarily large so that the index j on Ω_j and Λ_j is replaced by the continuous three-dimensional wavevector $\boldsymbol{k}$ (we note that the Lagrangian wave action spectrum is then given by $A_{\mathrm{L}}(\boldsymbol{k}) = \Lambda(\boldsymbol{k})/\Omega(\boldsymbol{k})$). The delta functions in (1.20) confine the system to the dispersion surface described by $\Omega(\boldsymbol{k})$ so that the system is wavelike. The three-dimensional wavenumber spectrum is obtained from (1.20) as

$$\hat{S}_{\mathrm{Ls}33}(\boldsymbol{k}) = \frac{1}{2\pi}\int \mathrm{d}\omega\, S_{\mathrm{Ls}33}(\boldsymbol{k},\omega) = \frac{k_{\mathrm{h}}^2 \Lambda(\boldsymbol{k})}{\rho k^2 \Omega^2(\boldsymbol{k})}, \tag{1.21}$$

and we find that the three-dimensional wavenumber spectrum is directly proportional to the Lagrangian energy distribution $\Lambda(\boldsymbol{k})$.

The role of statistical mechanics is to provide not only the form of the phase-space density function such as that given by (1.9), but also the Lagrangian energy distribution $\Lambda(\boldsymbol{k})$. From a knowledge of the system interactions it is, in principle, possible to derive a specific expression for $\Lambda(\boldsymbol{k})$. While our theoretical effort has not yet reached quite this level of maturity, it is an ultimate goal and certainly a direction for future efforts. Likewise, experimental efforts which measure the Lagrangian spectra, particularly wavenumber spectra, provide important information about the Lagrangian energy distribution $\Lambda(\boldsymbol{k})$ and stand in symbiotic relation to the corresponding theoretical efforts. In §3 we use the above outlined methods to calculate the four-dimensional Eulerian frequency wavenumber spectra and the corresponding three-dimensional Eulerian wavenumber spectra. We find that at small wavenumbers the Eulerian and Lagrangian spectra are approximately equal, but at large wavenumbers they are significantly different. At large wavenumbers the Eulerian spectra exhibit a power-law decay whose functional form is independent of $\Lambda(\boldsymbol{k})$ and whose scaling depends only upon an integral involving $\Lambda(\boldsymbol{k})$. This means that we do not need to know the precise details of $\Lambda(\boldsymbol{k})$ in order to make reasonable estimates of the Eulerian spectra. On the other hand, this also means that experiments which measure the decaying part of the Eulerian wavenumber spectrum cannot provide the details of $\Lambda(\boldsymbol{k})$ and, hence, cannot provide detailed information about the true dynamics of the system.

While we cannot yet provide a rigorous derivation of $A(\boldsymbol{k})$, we can propose a plausible form whose important features are clearly related to physical processes. In §2 we propose the form

$$A(\boldsymbol{k}) = E_0 \exp\{-\tfrac{1}{2}[\mu_h^2 k_h^2 + \mu_v^2 k_3^2]\}, \tag{1.22}$$

where μ_h and μ_v are horizontal and vertical lengthscales at which the population of the linear modes is suppressed. We will argue that to an adequate approximation (1.22) describes a system at canonical equilibrium for which contributions from the nonlinear interactions from horizontal and vertical lengthscales larger than μ_h and μ_v are negligible, but for which contributions from the nonlinear interactions from horizontal and vertical lengthscales smaller than μ_h and μ_v are large. This corresponds to the linear energy being equipartitioned among the large-scale modes and suppressed at small scales. It is clear that strong nonlinear contributions will cause the occupation of the corresponding modes to be suppressed, but the specific form of that suppression or cutoff is not clear. However, we will show that the Eulerian spectra and some of the marginal Lagrangian spectra are not sensitive to the specific form of the cutoff and that for this purpose the only important feature of (1.22) is the introduction of the lengthscales μ_h and μ_v at which the contributions from small horizontal and vertical lengthscales are suppressed. The Gaussian form has been chosen for mathematical convenience only and any other choice which introduces lengthscale cutoffs will produce essentially the same results. Once the level E_0 has been specified it should, in principle, be possible to compute the lengthscales μ_h and μ_v from a knowledge of the nonlinear interactions. While this is an important problem for future investigation, it is beyond the scope of this paper. Instead, by treating the three parameters E_0, μ_h, and μ_v as adjustable we obtain expressions for a wide variety of Eulerian spectra which are in striking agreement with experiment. These results along with a more detailed discussion are given in §4.

In this paper we establish a clear theoretical relationship between the Lagrangian energy distribution $A(\boldsymbol{k})$ and the observed Eulerian spectra. We also demonstrate that the observed spectra are consistent with the hypothesis that the ocean is at canonical equilibrium with the modes which correspond to small horizontal and vertical lengthscales suppressed due to strong nonlinear interactions. If this hypothesis could be rigorously established, then it would provide a first-principles explanation for the GM model. Our efforts fall somewhat short of this for two reasons. First, we do not actually derive an expression for $A(\boldsymbol{k})$ from a knowledge of the system interactions, but instead hypothesize a plausible form and demonstrate consistency. Secondly, the observed Eulerian spectra are quite insensitive to the details of $A(\boldsymbol{k})$ so that a variety of other forms for $A(\boldsymbol{k})$ will lead to similar results. The important contribution of this paper is to clarify the relationship between the observed Eulerian spectra and the fundamental dynamical processes which are most directly described in the Lagrangian frame. We bring into clear focus the important areas for theoretical study, namely the derivation of the Lagrangian energy distribution $A(\boldsymbol{k})$ from a knowledge of the system interactions and establishing more rigorously that the effects of strong nonlinear interactions can be approximated by the phase-space density function given by (1.9) with $A(\boldsymbol{k})$ given by (1.22) or some equivalent form. We also bring into clear focus the fact that experiments which measure the decaying part of the Eulerian wavenumber spectrum do not provide direct information about the important dynamical processes. A more detailed discussion of these points along with some suggestions for future efforts are given in the last section.

2. The Lagrangian spectra

In this section we obtain expressions for the Lagrangian frequency wavenumber spectra and for several one-dimensional marginal spectra which correspond to typical experiments. We then discuss the relationship between these and the distribution of energy among the linear internal wave modes. Later it will be shown that, for certain reasonable choices of the parameters μ_h and μ_v, the one-dimensional marginal spectra which are associated with moored measurements are in excellent qualitative agreement with experiment.

In this paper we shall make the Boussinesq approximation, that is we consider the fluid density ρ to be constant except for the purpose of computing the Väisälä profile which we will take to be the constant N. We also neglect the horizontal component of the Earth's rotation and assume that the Coriolis vector $\boldsymbol{f}$, which is of magnitude f, is vertical (for a formulation of this problem in terms of Lagrangian variables see e.g. Tolstoy 1963). We will initially use periodic boundary conditions in the vertical as well as the horizontal. Later we will treat surface effects as the need arises. Under these conditions the expressions given by (1.1) and (1.2) can be explicitly written as

$$\boldsymbol{s}_L(\boldsymbol{r},t) = \sum_{j=-M}^{M} \frac{1}{(2V\rho\Omega_j)^{\frac{1}{2}}}\left\{\left[\frac{l_{jh}}{l_j}\hat{\boldsymbol{r}}_3 - \frac{l_{j3}}{l_j}\hat{\boldsymbol{l}}_{jh}\right]q_j(t) - \frac{fl_{j3}}{\Omega_j l_j}\hat{\boldsymbol{n}}_j p_j(t)\right\}\exp\{i\boldsymbol{l}_j\cdot\boldsymbol{r}\}, \tag{2.1}$$

and

$$\boldsymbol{v}_L(\boldsymbol{r},t) = \sum_{j=-M}^{M} \frac{1}{(2V\rho\Omega_j)^{\frac{1}{2}}}\left\{\left[\frac{l_{jh}}{l_j}\hat{\boldsymbol{r}}_3 - \frac{l_{j3}}{l_j}\hat{\boldsymbol{l}}_{jh}\right]\Omega_j p_j(t) + \frac{fl_{j3}}{l_j}\hat{\boldsymbol{n}}_j q_j(t)\right\}\exp\{i\boldsymbol{l}_j\cdot\boldsymbol{r}\}, \tag{2.2}$$

where we have used a complex representation and altered the labelling system so that the number of degrees of freedom is now $2M+1$. In (2.1) and (2.2) the dispersion relation is given by

$$\Omega_j = \frac{(N^2 l_{jh}^2 + f^2 l_{j3}^2)^{\frac{1}{2}}}{l_j}. \tag{2.3}$$

V is the volume of the ocean, $\boldsymbol{l}_j$ is a three-dimensional wavevector of magnitude l_j, $\boldsymbol{l}_{jh}$ is the horizontal component of $\boldsymbol{l}_j$, l_{jh} is the magnitude of $\boldsymbol{l}_{jh}$, $\hat{\boldsymbol{l}}_{jh}$ is a unit vector in the direction $\boldsymbol{l}_{jh}$, l_{j3} is the vertical component of $\boldsymbol{l}_j$, r_3 is the vertical component of $\boldsymbol{r}$, $\hat{\boldsymbol{r}}_3$ is a vertical unit vector, and the unit vector $\hat{\boldsymbol{n}}_j = \hat{\boldsymbol{r}}_3 \times \hat{\boldsymbol{l}}_{jh}$. The eigenfunctions $\phi_{j\alpha}(\boldsymbol{r})$ are proportional to complex exponentials and, thus, the $p_j(t)$ and $q_j(t)$ are also complex. The vertical component of $\boldsymbol{l}_j$ is given by a positive or negative integer times $2\pi/D$ where D is the depth of the ocean and the horizontal components of $\boldsymbol{l}_j$ are given by positive or negative integers multiplied by $2\pi/A^{\frac{1}{2}}$ where A is the surface area of the ocean. For now we will consider the volume V of the ocean to be finite but will later allow it to become arbitrarily large. We shall designate the labelling system such that $\boldsymbol{l}_{-j} = -\boldsymbol{l}_j$ and we must therefore require that

$$q_{-j}(t) = q_j^*(t), \tag{2.4}$$

and

$$p_{-j}(t) = p_j^*(t). \tag{2.5}$$

The specific coefficients in (2.1) and (2.2) have been chosen so that the quadratic part of the Hamiltonian is given by

$$H_0(p,q) = \sum_{j=-M}^{M} \tfrac{1}{4}\Omega_j[p_j p_j^* + q_j q_j^*] = \sum_{j=1}^{M}\sum_{m=1}^{2} \tfrac{1}{2}\Omega_j[p_{jm}^2 + q_{jm}^2], \tag{2.6}$$

where we have suppressed explicit display of the time and since the term for which

$j = 0$ corresponds to a uniform translation of the system it has been omitted from the second expression in (2.6). We note that because of the conditions given by (2.4) and (2.5) the displacement and momentum associated with a given negative value of j are not independent of those associated with the corresponding positive value of j. Thus the second expression of (2.6) has been written in terms of real independent displacements and the corresponding canonically conjugate momenta where q_{j1} and q_{j2} are the real and imaginary parts of the complex displacement q_j and likewise p_{j1} and p_{j2} are the real and imaginary parts of the complex momentum p_j. By using the real independent displacements and momenta in (2.6) the phase-space density function given by (1.9) can be written as

$$g(p,q) = \prod_{j=1}^{M} \prod_{m=1}^{2} \frac{\Omega_j}{2\pi\Lambda_j} \exp\left\{-\frac{\Omega_j}{2\Lambda_j}[p_{jm}^2 + q_{jm}^2]\right\}. \tag{2.7}$$

The expectation value of any function of the dynamical variables, say $F(p,q,t)$, is given by

$$E[F(p,q,t)] = \int F(p,q,t)\, g(p,q) \prod_{j=1}^{M} \prod_{m=1}^{2} \mathrm{d}p_{jm}\, \mathrm{d}q_{jm}. \tag{2.8}$$

By using (2.7) and (2.8) it is easy to show that

$$E[p_{jm}\, p_{j'm'}] = \frac{\Lambda_j}{\Omega_j} \delta_{jj'} \delta_{mm'}, \tag{2.9}$$

$$E[q_{jm}\, q_{j'm'}] = \frac{\Lambda_j}{\Omega_j} \delta_{jj'} \delta_{mm'}, \tag{2.10}$$

and

$$E[p_{jm}\, q_{j'm'}] = 0. \tag{2.11}$$

These expressions can now be used to compute the various Lagrangian spectra.

In the following calculations we will have recurring need for the Cartesian components of (2.1) at both the times t and $t+\tau$. We will also make the weak interaction approximation so that the short-time dependence is well approximated by (1.14) and (1.15). By using (1.14), (1.15) and (2.1) along with

$$\hat{\boldsymbol{l}}_{jh} = \frac{l_{j1}\hat{\boldsymbol{r}}_1 + l_{j2}\hat{\boldsymbol{r}}_2}{l_{jh}}, \tag{2.12}$$

and

$$\hat{\boldsymbol{n}}_{jh} = -\frac{l_{j2}\hat{\boldsymbol{r}}_1 - l_{j1}\hat{\boldsymbol{r}}_2}{l_{jh}}, \tag{2.13}$$

we can write

$$\begin{aligned} \boldsymbol{s}_{\mathrm{L}}(\boldsymbol{r}, t+\tau) = \\ \sum_{j=-M}^{M} \frac{1}{(2V\rho\Omega_j)^{\frac{1}{2}}} \Bigg\{ \Bigg[\frac{l_{jh}}{l_j} \cos(\Omega_j \tau)\, \hat{\boldsymbol{r}}_3 - \frac{l_{j3}}{l_j l_{jh}} \left(l_{j1} \cos(\Omega_j \tau) + \frac{f l_{j2}}{\Omega_j} \sin(\Omega_j \tau) \right) \hat{\boldsymbol{r}}_1 \\ - \frac{l_{j3}}{l_j l_{jh}} \left(l_{j2} \cos(\Omega_j \tau) - \frac{f l_{j1}}{\Omega_j} \sin(\Omega_j \tau) \right) \hat{\boldsymbol{r}}_2 \Bigg] q_j(t) \\ + \Bigg[\frac{l_{jh}}{l_j} \sin(\Omega_j \tau)\, \hat{\boldsymbol{r}}_3 - \frac{l_{j3}}{l_j l_{jh}} \left(l_{j1} \sin(\Omega_j \tau) - \frac{f l_{j2}}{\Omega_j} \cos(\Omega_j \tau) \right) \hat{\boldsymbol{r}}_1 \\ - \frac{l_{j3}}{l_j l_{jh}} \left(l_{j2} \sin(\Omega_j \tau) + \frac{f l_{j1}}{\Omega_j} \cos(\Omega_j \tau) \right) \hat{\boldsymbol{r}}_2 \Bigg] p_j(t) \Bigg\} \exp\{i \boldsymbol{l}_j \cdot \boldsymbol{r}\}. \end{aligned} \tag{2.14}$$

We can now use (2.14) to compute any of the various Lagrangian correlation functions. Since we have taken the Väisälä profile to be constant and are neglecting surface effects, these correlation functions and the corresponding spectra are homogeneous in the vertical as well as the horizontal. As an illustration we shall consider the correlation function associated with the vertical displacement which is denoted by $C_{\mathrm{Ls33}}(\boldsymbol{R},\tau)$. By using (1.12), (2.9)–(2.11), (2.14), and by allowing V to become arbitrarily large we find

$$C_{\mathrm{Ls33}}(\boldsymbol{R},\tau)=\frac{1}{(2\pi)^3\rho}\int \mathrm{d}^3l\,\frac{l_{\mathrm{h}}^2\,A(\boldsymbol{l})}{l^2\Omega^2(\boldsymbol{l})}\cos\left(\Omega(\boldsymbol{l})\,\tau\right)\cos\left(\boldsymbol{l}\cdot\boldsymbol{R}\right). \tag{2.15}$$

Then by using (1.13) and (2.15) we obtain

$$S_{\mathrm{Ls33}}(\boldsymbol{k},\omega)=\frac{\pi k_{\mathrm{h}}^2\,A(\boldsymbol{k})}{\rho k^2\Omega^2(\boldsymbol{k})}\left[\delta(\Omega(\boldsymbol{k})-\omega)+\delta(\Omega(\boldsymbol{k})+\omega)\right], \tag{2.16}$$

for the full four-dimensional frequency wavenumber spectrum. The delta functions in (2.16) confine the system to the dispersion surface and the spectrum is, therefore, wavelike. The various marginal spectra can now be obtained from (2.16). For example, the three-dimensional wavenumber spectrum denoted by $\hat{S}_{\mathrm{Ls33}}(\boldsymbol{k})$ is obtained by integrating (2.16) over all frequencies to obtain

$$\hat{S}_{\mathrm{Ls33}}(\boldsymbol{k})=\frac{1}{2\pi}\int \mathrm{d}\omega\,S_{\mathrm{Ls33}}(\boldsymbol{k},\omega)=\frac{k_{\mathrm{h}}^2\,A(\boldsymbol{k})}{\rho k^2\Omega^2(\boldsymbol{k})}. \tag{2.17}$$

We note that the spectrum given by (2.17) is directly proportional to the Lagrangian energy distribution $A(\boldsymbol{k})$.

It is clear from (2.16) and (2.17) that the Lagrangian energy distribution $A(\boldsymbol{k})$ plays a crucial role in our description of the various Lagrangian spectra. It should in principle be possible to derive $A(\boldsymbol{k})$ from a knowledge of the system interactions. While this is an ultimate goal and important for a full understanding of the underlying physics, it is beyond our present capabilities. We can, however, determine some qualitative features of $A(\boldsymbol{k})$ and show that this is sufficient to gain at least a partial understanding of the observed spectra. Our treatment in this paper has made important use of the weak interaction approximation both through the use of (1.14) and (1.15) for short-time evolution and through the use of (2.7) for the phase-space density function. We now need to consider in more detail the conditions for the validity of the weak interaction approximation. The Hamiltonian given by (1.3) can also be written in the form

$$H(p,q)=T(p,q)+V(p,q), \tag{2.18}$$

where $T(p,q)$ is the kinetic energy and $V(p,q)$ is the full potential energy. The potential energy can be written in the form

$$V(p,q)=V_0(p,q)+V_1(p,q)=\int \mathrm{d}^3r\,U(p,q,\boldsymbol{r}), \tag{2.19}$$

where $V_0(p,q)$ is the quadratic part of the potential energy and $U(p,q,\boldsymbol{r})$ is the full potential energy density. It is important to realize that $U(p,q,\boldsymbol{r})$ is a density in terms of the Lagrangian label $\boldsymbol{r}$ and must be expressed in terms of Lagrangian variables. It can be shown that the potential energy density for a vertically stratified compressible fluid is given by

$$U=P(z+s_{\mathrm{L3}})\,J(\boldsymbol{s}_{\mathrm{L}})-P(z)-\frac{\partial P(z)}{\partial z}s_{\mathrm{L3}}+\frac{P(z)}{(\gamma-1)}\left[\frac{1}{[J(\boldsymbol{s}_{\mathrm{L}})]^{(\gamma-1)}}-1\right], \tag{2.20}$$

where we have assumed that expansion and compression of the fluid takes place adiabatically. In (2.20) we have suppressed the display of the dynamical variables (p, q), $P(z)$ is the static pressure at the vertical position z, and γ is the ratio of the specific heat at constant pressure to the specific heat at constant volume. We note that in the static or undisturbed condition $s_L = 0$ so that the Lagrangian label $\boldsymbol{r}$ and the Eulerian label $\boldsymbol{x}$ are equal and $z = r_3 = x_3$ is the vertical component of either the Lagrangian or the Eulerian label.

The form of the interaction potential required in (1.3) is obtained by expanding the term $P(z+s_{L3})$ in (2.20) about $s_{L3} = 0$ and the term $1/[J(s_L)]^{\gamma-1}$ about $J(s_L) = 1$. The quadratic terms are included in $V_0(p, q)$ while the cubic and higher-order terms comprise the interaction potential $V_1(p, q)$. By making the above expansion the quadratic part of the potential energy density U_0 is found to be given by

$$U_0 = \tfrac{1}{2}\rho(z)\{[N^2(z)+g^2/c^2(z)]\, s_{L3}^2 + c^2(z)\,[\nabla\cdot\boldsymbol{s}_L]^2 - 2g s_{L3}\,\nabla\cdot\boldsymbol{s}_L\}, \tag{2.21}$$

where $\rho(z)$ is the static fluid density, $N(z)$ is the Väisälä profile defined by

$$N^2(z) = -g\left[\frac{1}{\rho(z)}\frac{\partial\rho(z)}{\partial z} + \frac{g}{c^2(z)}\right], \tag{2.22}$$

g is the acceleration due to gravity, $c(z)$ is the speed of sound defined by

$$c^2(z) = \frac{\gamma P(z)}{\rho(z)}, \tag{2.23}$$

and we have used the fundamental law of hydrostatics which is given by

$$\frac{\partial P(z)}{\partial z} = -g\rho(z). \tag{2.24}$$

We note that the expression for U_0 given by (2.21) is the same as that obtained by Tolstoy (1963). In order that these expansions converge we must limit both the size of the vertical component of the displacement and the size of the various spatial derivatives of all components of the displacement. For non-compressional gravity waves $\nabla\cdot\boldsymbol{s}_L$ is of order $1/c^2(z)$, which may be considered small, but other combinations of spatial derivatives are not so constrained. In order to satisfy these limitations we must limit not only the average energy per mode but also the modal bandwidth. If the modes are occupied out to arbitrarily small lengthscales, then both the free-field energy and the nonlinear contributions from the interaction potential will be arbitrarily large. It can be shown that the nonlinear energy grows much more rapidly as a function of decreasing lengthscale than does the free-field or linear energy. Thus, strong nonlinear interactions will ultimately limit the participation of small lengthscales.

The above class of interactions will be referred to as internal interactions since they are present even when the system is isolated. Interactions with the outside world, such as those associated with sources and sinks of energy, will be referred to as external interactions. We shall consider a hierarchy of three cases which correspond to progressively greater levels of excitation as well as different relative strengths of the internal and external interactions. The first case, which is the most simple and best known, is that for which the external interactions are negligible (i.e. the input and dissipation of energy is negligible) and the level of excitation is small enough to consider all internal nonlinear interactions as weak. In this case energy is

redistributed among the linear modes by weak internal interactions until the system reaches canonical equilibrium where energy is equipartitioned across the accessible modes. In order to limit the modal band width we shall consider that molecular viscosity provides an absolute lower bound to the participation of the small-scale modes. While we will find, for internal waves, that processes other than molecular viscosity are more important for limiting the participation of the small-scale modes, it still provides an absolute lower bound and a useful base line for comparison to the other two cases. The second case is that for which the timescales associated with external interactions (i.e. energy input and dissipation) are comparable to or shorter than those associated with internal interactions and the level of excitation, while greater than for the first case, is still small enough to treat the internal interactions as weak. The third case is that for which the internal interactions dominate so that the timescales associated with internal interactions are shorter than those associated with external interactions and are important at lengthscales which are much greater than those associated with molecular viscosity. We shall now consider these three cases in greater detail.

We will find it convenient to write the average energy per mode in the form

$$\Lambda_j = E_0 h_j, \tag{2.25}$$

where E_0 is the maximum average energy per mode and h_j is a dimensionless (convergence) factor which provides the structure of the modal occupation and more importantly cuts off the participation of the modes which correspond to small lengthscales. In geophysical fluids, such as the ocean, molecular viscosity provides a fundamental basis for excluding the small-scale modes. In a typical situation the modes which correspond to lengthscales shorter than about a millimetre are strongly damped and are, thus, ineffective for storing energy. We can, therefore, think of a minimum lower bound μ_m (i.e. μ_m is on the order of 1 mm) for the lengthscale cutoff provided by molecular viscosity. If, for example, we consider a system for which the internal interactions dominate, then we would expect the system to evolve near to canonical equilibrium so that the phase-space density function is given by (2.7) with $\Lambda_j = E_0$ and with the number of degrees of freedom limited to lengthscales greater than μ_m by molecular viscosity. In this case the convergence factor h_j is unity for modes which correspond to lengthscales greater than μ_m and then decreases rapidly to zero for modes which correspond to lengthscales smaller than μ_m. We must restrict E_0 to be small enough to assure that the nonlinear contributions are negligible, but if this condition is met, then (2.7) can be used for the calculation of statistical averages. We shall refer to this scenario as case I.

The second case to be considered involves external interactions. While the Prigogine (1962) formulation is for an isolated system, there exist other treatments that allow the inclusion of additional degrees of freedom which can be used to represent generation and dissipation mechanisms. For example, Mori (1965) has cast the problem in the form of a generalized Langevin equation which can be used for this purpose. The application of Langevin methods to the oceanic internal wave system has been considered by Pomphrey, Meiss & Watson (1980) who argue that the GM spectrum corresponds to a minimum in the energy transfer rates. Unfortunately, these, as well as other oceanographic studies (Pomphrey 1981; Holloway 1981), have not in general resulted in an improved understanding of the role of generation and dissipation mechanisms. Indeed, it seems clear that the reason for this is that none of these studies has introduced a model for generation and dissipation which is

sufficiently detailed to have been able to provide such an improved understanding. This shortcoming has been partially addressed by West (1982) who considers a set of test waves which interact among themselves and with an additional set of waves which are referred to as a heat bath. The term 'heat bath' simply means that the additional set of waves is large in comparison to the set of test waves so that it can be considered to be a reservoir which supplies energy to or absorbs energy from the test waves without being significantly affected by them. West obtains a generalized Langevin equation, the associated Fokker–Planck equation, and shows that the steady-state solution for the distribution of test waves depends upon the assumed distribution of heat-bath waves. Specifically it is shown that the steady-state phase-space density function for the distribution of the canonically conjugate test-wave variables is given by

$$g(p,q) = (1/Z)\exp\left\{-\sum_{j=1}^{M}\sum_{m=1}^{2}[(\tfrac{1}{2}\Omega_j)(p_{jm}^2+q_{jm}^2)+V_{Ijm}(p,q)]/\Lambda_j\right\}, \tag{2.26}$$

where the interaction potential has been written in the form

$$V_I(p,q) = \sum_{j=1}^{M}\sum_{m=1}^{2} V_{Ijm}(p,q), \tag{2.27}$$

and Λ_j in general depends upon the distribution of heat-bath variables.

Prigogine & Henin (1957, 1960) have considered the case of strong nonlinear interactions in isolated systems. They obtain a generalized master equation and show that its long-time solutions correspond to canonical equilibrium. In this case the phase-space density function is given by (2.26) with $\Lambda_j = E_0$ so that the average energy of the jth mode is independent of the mode index but in general the interaction potential must also be included. Thus, (2.26) can be viewed as a generalization of canonical equilibrium which includes the possibility of interactions with a generalized heat bath as well as the possibility of strong nonlinear internal interactions. In all realistic situations both types of interactions are present. The crucial issue is which of the two types of interaction dominates the time evolution of the phase-space density function. If internal interactions dominate, then we would expect the phase-space density function to evolve near to the canonical distribution (i.e. (2.26) with $\Lambda_j = E_0$). If external interactions dominate, then we would expect the more general distribution given by (2.26) with Λ_j determined by the heat bath. We point out here that the inclusion of external interactions does not preclude the possibility of obtaining the canonical distribution. While it is never explicitly stated by West (1982), it is clear from his results (see his equation (3.18)) that if the heat-bath waves are distributed in accordance with the canonical distribution, then the test waves are also distributed in accordance with the canonical distribution. Thus we may view the canonical distribution as a special case of (2.26) which is obtained if either the external interactions are negligible in comparison to the internal interactions of if the heat bath is distributed in accordance with the canonical distribution.

If we now consider a system for which external interactions dominate, then we would expect the phase-space density function given by (2.26) where Λ_j must be such that the modes excluded by molecular viscosity are not populated but otherwise it is determined by the heat bath (i.e. energy input and dissipation). In this case the heat bath provides the lengthscale cutoffs μ_h and μ_v. We point out here that our use

of the word cutoff does not necessarily imply an abrupt cutoff. For example, the convergence factor h_j might be such that it exhibits a strong power-law decay for modes which correspond to horizontal lengthscales smaller than μ_h and vertical lengthscales smaller than μ_v. We shall find it convenient to introduce a new horizontal lengthscale ν_h and vertical lengthscale ν_v which are equal to the root-mean-square (r.m.s.) horizontal Lagrangian displacement and the r.m.s. vertical Lagrangian displacement, respectively. We will find that these r.m.s. lengthscales play an important role in the development of the Eulerian spectra and therefore refer to them as Eulerian lengthscales. It can be shown that ν_h and ν_v are given by

$$\nu_v \propto \left(\frac{E_0}{N^2\rho\mu_h^2\mu_v}\right)^{\frac{1}{3}} \propto \frac{\nu_h\mu_v}{\mu_h}, \tag{2.28}$$

where the factors of proportionality are of order unity. The first expression of (2.28) follows from equipartitioning energy out to the lengthscale μ_v in a vertically stratified fluid, while the second expression depends upon the relation between the vertical and horizontal components of the linear internal wave eigenfunctions. Both expressions are derived in Appendix A. It is also shown in Appendix A that the ratios $\nu_h/\mu_h \approx \nu_v/\mu_v$ must be limited for the weak interaction approximation to be valid. If these conditions are met, then (2.26) can be replaced by (2.7) for the calculation of statistical averages. It is this scenario which has been proposed by McComas & Müller (1981). Thus, it is assumed that generation and dissipation mechanisms provide a heat bath which establishes the convergence factor h_j such that the GM action spectrum is obtained. However, such a proposal simply transfers our lack of understanding to the heat bath, the detailed nature of which must eventually be explained. In the case of oceanic internal waves the precise details of generation and dissipation mechanisms are not completely known, but what is known does not seem to lead to an explanation for the quasi-universal character of the GM spectrum (Holloway 1986). Further, existing estimates of the evolution rates due to internal and external interactions seem to suggest that at most lengthscales of interest the internal interaction rates are much larger than the external interaction rates. While this proposal has some attractive features there are also some important unresolved issues. We shall refer to this scenario as case II.

A third scenario which is the most intriguing is also the most speculative. We now consider a system which is near canonical equilibrium but for which we cannot make the weak-interaction approximation. The phase-space density function is given by (2.26) with $A_j = E_0$ but in general the interaction potential cannot be neglected. In this case the exact expression given by (2.26) is usually not tractable. In Appendix A it is shown that for a given amplitude of displacement the modes which correspond to small lengthscales contribute much more strongly to the nonlinear interaction energy than do the modes which correspond to larger lengthscales. Thus, realizations of the system for which the small lengthscales are significantly populated are more energetic than realizations for which large lengthscales are correspondingly populated, and due to the form of the phase-space density function given by (2.26) are much less likely to occur. In this case the form of the phase space density function provides a basis for the exclusion of the small-scale modes. We can approximate (2.26) by (2.7) if we choose A_j such that $A_j = E_0$ for modes which correspond to horizontal lengthscales larger than μ_h and vertical lengthscales larger than μ_v and then decreases rapidly to zero for smaller lengthscales.

To illustrate this we note that the argument of the exponential factor in (2.26) can be written as

$$\frac{H(p,q)}{E_0} = \sum_{j=1}^{M}\sum_{m=1}^{2}[(\tfrac{1}{2}\Omega_j)(p_{jm}^2+q_{jm}^2)+V_{1jm}(p,q)]/E_0$$

$$= \sum_{j=1}^{M}\sum_{m=1}^{2}\left[(\tfrac{1}{2}\Omega_j)(p_{jm}^2+q_{jm}^2)\frac{[1+V_{1jm}(p,q)/H_{0jm}(p,q)]}{E_0}\right], \tag{2.29}$$

where

$$H_{0jm}(p,q) = (\tfrac{1}{2}\Omega_j)(p_{jm}^2+q_{jm}^2). \tag{2.30}$$

We can now define an effective energy for the jth mode $\hat{A}_{jm}(p,q)$ such that

$$\hat{A}_{jm}(p,q) = \frac{E_0}{[1+V_{1jm}(p,q)/H_{0jm}(p,q)]}, \tag{2.31}$$

and write the phase-space density function in a form which looks similar to (2.7). There is, however, an important difference between $\hat{A}_{jm}(p,q)$ and the average energy of the jth mode, A_j, in (2.7). The parameter A_j does not depend upon the p_{jm} and q_{jm}, while $\hat{A}_{jm}(p,q)$ does. Obviously (2.26) is in general non-Gaussian and no amount of manipulation can change this. However, if the nonlinear interaction energy associated with a given mode is small relative to the free-field energy associated with that mode, then (2.31) yields approximately the constant E_0. On the other hand, if the nonlinear interaction energy associated with a given mode is much larger than the free-field energy associated with that mode, then (2.31) yields a result much smaller than E_0 and because of the form of (2.26) these modes are much less likely to be occupied. We have approximated this situation by replacing (2.31) by an average value and assumed that the average rapidly approaches zero for lengthscales which are smaller than μ_h or μ_v. Such an approximation is qualitatively reasonable, but cannot be expected to provide detailed quantitative information about the exclusion of the small-scale modes. If it were our goal to obtain precise information about the three-dimensional Lagrangian wavenumber spectrum which is directly proportional to $A(\boldsymbol{k})$, then this would be a serious shortcoming. However, we will find that the various Eulerian spectra as well as the marginal Lagrangian spectra associated with moored measurements are not sensitive to these details and, therefore, this approximation is adequate for our purposes here. The Eulerian lengthscales given by (2.28) also play an important role in this scenario and we must require that the ratios $\nu_h/\mu_h \approx \nu_v/\mu_v$ be limited in order to neglect the interaction potential in the region for which (2.31) is approximately equal to E_0. If these conditions are met, then (2.7) can be used for the calculation of statistical averages. We shall refer to this scenario as case III. The cutoff proposed in case III is equivalent to arguments concerning the breakdown of internal waves due to local instabilities at small Richardson number (Phillips 1969).

The one-dimensional Lagrangian frequency spectrum $\bar{S}_{Ls33}(\omega)$ is defined as an integral of the four-dimensional Lagrangian frequency wavenumber spectrum over all wavenumbers. By using (2.16) we can write

$$\bar{S}_{Ls33}(\omega) = \frac{1}{(2\pi)^3}\int \mathrm{d}^3k S_{Ls33}(\boldsymbol{k},\omega) = \frac{1}{8\pi^2\rho}\int \mathrm{d}^3k \frac{k_h^2 A(\boldsymbol{k})}{k^2\Omega^2(\boldsymbol{k})}[\delta(\Omega(\boldsymbol{k})-\omega)+\delta(\Omega(\boldsymbol{k})+\omega)]. \tag{2.32}$$

If we now assume that $A(\boldsymbol{k})$ is isotropic in the horizontal, then two of the integrals in (2.32) can be evaluated. By using (2.3) to write

$$k_3(k_\mathrm{h}, \Omega) = k_\mathrm{h}\left(\frac{N^2-\Omega^2}{\Omega^2-f^2}\right)^{\frac{1}{2}}, \tag{2.33}$$

the integral over k_3 in (2.32) can be transformed to an integral over Ω and by using polar coordinates in the horizontal we find

$$\bar{S}_{\mathrm{Ls33}}(\omega) = \frac{1}{2\pi\rho\omega(N^2-\omega^2)^{\frac{1}{2}}(\omega^2-f^2)^{\frac{1}{2}}}\int_0^\infty \mathrm{d}k_\mathrm{h}\, k_\mathrm{h}^2\, A(k_\mathrm{h}, k_3(k_\mathrm{h}, \omega)). \tag{2.34}$$

It is clear from (2.34) that this frequency spectrum is not sensitive to the details of $A(\boldsymbol{k})$. To see this we write

$$A(\boldsymbol{k}) = E_0\, h(\boldsymbol{k}) = E_0\, h((\mu_\mathrm{h}^2 k_\mathrm{h}^2 + \mu_\mathrm{v}^2 k_3^2)^{\frac{1}{2}}), \tag{2.35}$$

where $h(x)$ is any function which exhibits reasonable convergence properties at large x. By using (2.35) in (2.34) and making the change of variables

$$x = k_\mathrm{h}\left(\frac{\mu_\mathrm{h}^2(\omega^2-f^2)+\mu_\mathrm{v}^2(N^2-\omega^2)}{(\omega^2-f^2)}\right)^{\frac{1}{2}} \tag{2.36}$$

we find

$$\bar{S}_{\mathrm{Ls33}}(\omega) = \frac{E_0(\omega^2-f^2)}{2\pi\rho\omega(N^2-\omega^2)^{\frac{1}{2}}([\mu_\mathrm{h}^2(\omega^2-f^2)+\mu_\mathrm{v}^2(N^2-\omega^2)]^3)^{\frac{1}{2}}}\int_0^\infty \mathrm{d}x x^2\, h(x). \tag{2.37}$$

The integral in (2.37) is insensitive to the details of the convergence factor $h(\boldsymbol{k})$. Other than to provide convergence $h(\boldsymbol{k})$ affects only the overall scaling and then only in terms of its second moment. We will find that most other spectra which are normally compared to experiment (these are mostly Eulerian) also exhibit a weak dependence upon the details of the convergence factor (i.e. dependence upon low-order moments). For practical purposes it matters little if $h(\boldsymbol{k})$ provides convergence by inverse power law, exponential, Gaussian, or infinitely many other forms. If we were able to measure the Lagrangian wavenumber spectrum given by (2.17), then we would have a direct measure of the convergence factor $h(\boldsymbol{k})$. However, as we will see later, none of the usual experiments accomplishes this and for our purposes here it makes no difference how $h(\boldsymbol{k})$ is chosen. In this paper we will choose

$$h(\boldsymbol{k}) = \exp\{-\tfrac{1}{2}[\mu_\mathrm{h}^2 k_\mathrm{h}^2 + \mu_\mathrm{v}^2 k_3^2]\}, \tag{2.38}$$

which results in the value $(\frac{1}{2}\pi)^{\frac{1}{2}}$ for the integral in (2.37). This choice is for mathematical convenience only and many other choices will yield entirely similar results.

The expression for the one-dimensional frequency spectrum given by (2.37) exhibits excellent qualitative agreement with experiment. If $\mu_\mathrm{v} \ll \mu_\mathrm{h}$ (this is a reasonable requirement), then for most frequencies (2.37) exhibits the characteristic $1/\omega^2$ frequency dependence observed in experiments. Near the inertial frequency the spectrum given by (2.37) rises to a peak and then decreases rapidly to zero as ω approaches f from above. This behaviour is also consistent with experiment. As ω approaches N from below (2.37) exhibits an integrable singularity. While this differs somewhat from experiment, we will show that by using fixed-surface boundary conditions this singularity is converted into a bump which is similar to what which is observed experimentally.

The most appropriate boundary conditions are that the sea floor is rigid and the air–sea interface is free. The free-surface boundary condition leads to a transcendental equation for the internal wave dispersion relation and is not convenient for our purposes here. By using instead a rigid-surface boundary condition, we loose the surface wave mode but obtain an excellent approximation to the internal wave modes. If we use a fixed-surface boundary condition we obtain in place of (2.14) for the Lagrangian displacement

$$\begin{aligned}
s_{\mathrm{L}}(\boldsymbol{r}, t+\tau) = \sum_{j=-M}^{M} \frac{1}{(V\rho\Omega_j)^{\frac{1}{2}}} \Bigg\{ \Bigg[& \sin(l_{j3} r_3) \frac{l_{j\mathrm{h}}}{l_j} \cos(\Omega_j \tau)\, \hat{\boldsymbol{r}}_3 \\
& + \mathrm{i} \cos(l_{j3} r_3) \frac{l_{j3}}{l_j l_{j\mathrm{h}}} \left(l_{j1} \cos(\Omega_j \tau) + \frac{f l_{j2}}{\Omega_j} \sin(\Omega_j \tau) \right) \hat{\boldsymbol{r}}_1 \\
& + \mathrm{i} \cos(l_{j3} r_3) \frac{l_{j3}}{l_j l_{j\mathrm{h}}} \left(l_{j2} \cos(\Omega_j \tau) - \frac{f l_{j1}}{\Omega_j} \sin(\Omega_j \tau) \right) \hat{\boldsymbol{r}}_2 \Bigg] q_j(t) \\
& + \Bigg[\sin(l_{j3} r_3) \frac{l_{j\mathrm{h}}}{l_j} \sin(\Omega_j \tau)\, \hat{\boldsymbol{r}}_3 + \mathrm{i} \cos(l_{j3} r_3) \frac{l_{j3}}{l_j l_{j\mathrm{h}}} \left(l_{j1} \sin(\Omega_j \tau) - \frac{f l_{j2}}{\Omega_j} \cos(\Omega_j \tau) \right) \hat{\boldsymbol{r}}_1 \\
& + \mathrm{i} \cos(l_{j3} r_3) \frac{l_{j3}}{l_j l_{j\mathrm{h}}} \left(l_{j2} \sin(\Omega_j \tau) + \frac{f l_{j1}}{\Omega_j} \cos(\Omega_j \tau) \right) \hat{\boldsymbol{r}}_2 \Bigg] p_j(t) \Bigg\} \exp\{\mathrm{i} \boldsymbol{l}_{j\mathrm{h}} \cdot \boldsymbol{r}_{\mathrm{h}}\}.
\end{aligned} \tag{2.39}$$

We can now use (2.39) to compute any of the various Lagrangian correlation functions. As an illustration we shall consider the correlation function associated with the vertical displacement which is denoted by $C_{\mathrm{Ls33}}(\boldsymbol{r}, \boldsymbol{R}, \tau)$. By using (1.12), (2.7)–(2.11), and (2.39) we find

$$\begin{aligned}
C_{\mathrm{Ls33}}(\boldsymbol{r}, \boldsymbol{R}, \tau) &= \frac{E_0}{V\rho} \sum_{j=-M}^{M} \frac{h_j l_{j\mathrm{h}}^2}{l_j^2 \Omega_j^2} \cos(\Omega_j \tau) \cos(\boldsymbol{l}_{j\mathrm{h}} \cdot \boldsymbol{R}_{\mathrm{h}}) [\cos(l_{j3} R_3) - \cos(2 l_{j3} r_3)] \\
&= \frac{E_0}{(2\pi)^3 \rho} \int \mathrm{d}^3 l \frac{h(\boldsymbol{l}) l_{\mathrm{h}}^2}{l^2 \Omega^2(\boldsymbol{l})} \cos(\Omega(\boldsymbol{l}) \tau) \cos(\boldsymbol{l}_{\mathrm{h}} \cdot \boldsymbol{R}_{\mathrm{h}}) [\cos(l_3 R_3) - \cos(2 l_3 r_3)]
\end{aligned} \tag{2.40}$$

where in the last line of (2.40) we have taken the limit that V becomes arbitrarily large. We note that, since the second term within the bracket in (2.40) is proportional to the $\cos(2 l_3 r_3)$, this correlation function is not homogeneous in the vertical. In the GM model, as well as most other oceanographic studies, this inhomogeneous term is neglected. However, there are some interesting features associated with this term so for now it will be retained.

All of the marginal spectra associated with moored measurements of the vertical displacement can be obtained from the moored cross spectrum $\mathrm{MCS}_{\mathrm{Ls33}}(\boldsymbol{r}, \boldsymbol{R}, \omega)$ which is defined as the temporal Fourier transform of (2.40). By using (2.40) we find

$$\begin{aligned}
\mathrm{MCS}_{\mathrm{Ls33}}(\boldsymbol{r}, \boldsymbol{R}, \omega) &= \int_{-\infty}^{\infty} \mathrm{d}\tau\, C_{\mathrm{Ls33}}(\boldsymbol{r}, \boldsymbol{R}, \tau) \exp\{\mathrm{i}\omega\tau\} = \frac{E_0}{2\pi\rho} \int_0^{\infty} \mathrm{d}l_{\mathrm{h}} \int_0^{\infty} \mathrm{d}l_3 \frac{h(l_{\mathrm{h}}, l_3)\, l_{\mathrm{h}}^3}{l^2 \Omega^2(l_{\mathrm{h}}, l_3)} \\
&\quad \times J_0(l_{\mathrm{h}} R_{\mathrm{h}}) [\cos(l_3 R_3) - \cos(2 l_3 r_3)] [\delta(\omega - \Omega(l_{\mathrm{h}}, l_3)) + \delta(\omega + \Omega(l_{\mathrm{h}}, l_3))] \\
&= \frac{E_0}{2\pi\rho\omega(\omega^2 - f^2)^{\frac{1}{2}}(N^2 - \omega^2)^{\frac{1}{2}}} \int_0^{\infty} \mathrm{d}l_{\mathrm{h}}\, h(l_{\mathrm{h}}, l_3(l_{\mathrm{h}}, \omega))\, l_{\mathrm{h}}^2 J_0(l_{\mathrm{h}} R_{\mathrm{h}}) \\
&\quad \times [\cos(l_3(l_{\mathrm{h}}, \omega) R_3) - \cos(2 l_3(l_{\mathrm{h}}, \omega) r_3)],
\end{aligned} \tag{2.41}$$

where $J_0(x)$ is a Bessel function of zero order. In the second expression of (2.41) we have written the horizontal component of the wavevector in polar coordinates, assumed that the convergence factor is independent of the polar angle, and integrated over it. In the third expression of (2.41) we have used (2.33) to transform the integral over l_3 to an integral over Ω, and then evaluated the integral.

We shall illustrate these results by considering the moored vertical displacement autospectrum denoted by $\bar{S}_{\mathrm{Ls33}}(r_3,\omega)$, the moored vertical velocity autospectrum denoted by $\bar{S}_{\mathrm{Lv33}}(r_3,\omega)$, and the moored vertical coherence denoted by $\mathrm{MVC}_{\mathrm{Ls33}}(R_3, r_3,\omega)$. The moored vertical displacement autospectrum is obtained from (2.41) by setting $R_3 = R_{\mathrm{h}} = 0$ and using (2.38) to obtain

$$\mathrm{MS}_{\mathrm{Ls33}}(r_3,\omega) = \frac{E_0(\omega^2-f^2)[1-G(2r_3)]}{(8\pi)^{\frac{1}{2}}\rho\omega(N^2-\omega^2)^{\frac{1}{2}}(\mu_{\mathrm{h}}^2(\omega^2-f^2)+\mu_{\mathrm{v}}^2(N^2-\omega^2))^{\frac{3}{2}}}, \tag{2.42}$$

where

$$G(\chi) = \left\{1-\frac{(N^2-\omega^2)\chi^2}{[\mu_{\mathrm{h}}^2(\omega^2-f^2)+\mu_{\mathrm{v}}^2(N^2-\omega^2)]}\right\}\exp\left\{-\frac{(\tfrac{1}{2})(N^2-\omega^2)\chi^2}{[\mu_{\mathrm{h}}^2(\omega^2-f^2)+\mu_{\mathrm{v}}^2(N^2-\omega^2)]}\right\}. \tag{2.43}$$

The moored vertical velocity autospectrum is easily obtained from (2.42) by noting that

$$\bar{S}_{\mathrm{Lv33}}(r_3,\omega) = \omega^2\bar{S}_{\mathrm{Ls33}}(r_3,\omega). \tag{2.44}$$

Finally, the moored vertical coherence is defined as the ratio of the magnitude of the moored cross spectrum between two points separated by the vertical distance R_3 to the moored autospectrum. It is easily shown to be given by

$$\mathrm{MVC}_{\mathrm{Ls33}}(R_3, r_3,\omega) = \frac{|G(R_3)-G(2r_3)|}{[1-G(2r_3)]}. \tag{2.45}$$

A comparison between these expressions and experiment will be given in the fourth section where excellent qualitative agreement is obtained.

3. The Eulerian spectra

The definition of an Eulerian variable as a weighted average of the corresponding Lagrangian variable was introduced in (1.16). If $F_{\mathrm{L}}(\boldsymbol{r},t)$ is a Lagrangian variable, then the corresponding Eulerian variable $F_{\mathrm{E}}(\boldsymbol{x},t)$ is given by

$$F_{\mathrm{E}}(\boldsymbol{x},t) = \int \mathrm{d}^3r\, F_{\mathrm{L}}(\boldsymbol{r},t)\, W(\boldsymbol{x},\boldsymbol{r},t), \tag{3.1}$$

where the weighting function $W(\boldsymbol{x},\boldsymbol{r},t)$ is given by

$$W(\boldsymbol{x},\boldsymbol{r},t) = \delta(\boldsymbol{x}-\boldsymbol{y})\, J(\boldsymbol{s}). \tag{3.2}$$

The delta function in (3.2) can be expressed in terms of its Fourier transform such that

$$\delta(\boldsymbol{x}-\boldsymbol{y}) = \frac{1}{(2\pi)^3}\int \mathrm{d}^3m \exp\{\mathrm{i}\boldsymbol{m}\cdot(\boldsymbol{x}-\boldsymbol{y})\}. \tag{3.3}$$

By using (3.1) we can in principle compute any Eulerian quantity from the corresponding Lagrangian quantity. If the phase-space density function is given by (1.15), then exact expressions for the four-dimensional frequency wavenumber spectra associated with the Eulerian variables defined by (3.1) can always be obtained.

While the procedure we will use is straightforward, it often results in tedious calculations and it is helpful to make use of a compact notation. If we use (3.1)–(3.3) to obtain an expression for the Eulerian variable, then the complicating factors in that expression are the Jacobian determinant and the part of the complex exponential which depends upon the displacement. By making use of the perfectly antisymmetric tensor of the third rank $\epsilon_{\alpha\beta\gamma}$ we can write

$$J(\boldsymbol{s})\exp\{-\mathrm{i}\boldsymbol{m}\cdot\boldsymbol{y}\} = \sum_{\alpha=1}^{3}\sum_{\beta=1}^{3}\sum_{\gamma=1}^{3}\epsilon_{\alpha\beta\gamma}\left[\delta_{1\alpha}+\frac{\partial s_{\mathrm{L}1}(\boldsymbol{r},t)}{\partial r_\alpha}\right]\left[\delta_{2\beta}+\frac{\partial s_{\mathrm{L}2}(\boldsymbol{r},t)}{\partial r_\beta}\right]\left[\delta_{3\gamma}+\frac{\partial s_{\mathrm{L}3}(\boldsymbol{r},t)}{\partial r_\gamma}\right]$$

$$\times\exp\{-\mathrm{i}\boldsymbol{m}\cdot(\boldsymbol{r}+\boldsymbol{s}_{\mathrm{L}}(\boldsymbol{r},t))\} = \sum_{\alpha=1}^{3}\sum_{\beta=1}^{3}\sum_{\gamma=1}^{3}\epsilon_{\alpha\beta\gamma}\frac{\mathrm{i}^3}{m_1 m_2 m_3}\frac{\partial E_1}{\partial r_\alpha}\frac{\partial E_2}{\partial r_\beta}\frac{\partial E_3}{\partial r_\gamma}, \quad (3.4)$$

where
$$E_\alpha = \exp\{-\mathrm{i}m_\alpha[r_\alpha+s_{\mathrm{L}\alpha}(\boldsymbol{r},t)]\} \quad (1\leqslant\alpha\leqslant 3). \quad (3.5)$$

Then by using (3.1)–(3.5) the expression for the Eulerian variable can be written

$$F_{\mathrm{E}}(\boldsymbol{x},t) = \frac{1}{(2\pi)^3}\sum_{\alpha=1}^{3}\sum_{\beta=1}^{3}\sum_{\gamma=1}^{3}\epsilon_{\alpha\beta\gamma}\int\mathrm{d}^3r\int\mathrm{d}^3m\exp\{\mathrm{i}\boldsymbol{m}\cdot\boldsymbol{x}\}F_{\mathrm{L}}(\boldsymbol{r},t)\frac{\mathrm{i}^3}{m_1 m_2 m_3}\frac{\partial E_1}{\partial r_\alpha}\frac{\partial E_2}{\partial r_\beta}\frac{\partial E_3}{\partial r_\gamma}. \quad (3.6)$$

The product of the last three factors in (3.6) contains terms which are up to cubic order in the spatial derivatives of the displacements as well as a complex exponential factor which is a function of the displacement. If we integrate (3.6) by parts with respect to r_α, we will reduce by one the number of factors which contain spatial derivatives of the displacement and this results in a considerable simplification of the following statistical calculations. Thus, by integrating (3.6) by parts we obtain

$$F_{\mathrm{E}}(\boldsymbol{x},t) = \frac{-\mathrm{i}}{(2\pi)^3}\sum_{\alpha=1}^{3}\sum_{\beta=1}^{3}\sum_{\gamma=1}^{3}\epsilon_{\alpha\beta\gamma}\int\mathrm{d}^3r\int\mathrm{d}^3m\frac{1}{m_1}\exp\{\mathrm{i}\boldsymbol{m}\cdot(\boldsymbol{x}-\boldsymbol{r})\}$$

$$\times\frac{\partial F_{\mathrm{L}}(\boldsymbol{r},t)}{\partial r_\alpha}\left[\delta_{\beta 2}+\frac{\partial s_{\mathrm{L}2}(\boldsymbol{r},t)}{\partial r_\beta}\right]\left[\delta_{\gamma 3}+\frac{\partial s_{\mathrm{L}3}(\boldsymbol{r},t)}{\partial r_\gamma}\right]\exp\{-\mathrm{i}\boldsymbol{m}\cdot\boldsymbol{s}_{\mathrm{L}}(\boldsymbol{r},t)\}, \quad (3.7)$$

where we have also used (3.5).

For our purposes in this paper we shall consider the vertical displacement which by using (3.7) and the properties of $\epsilon_{\alpha\beta\gamma}$ can be written

$$s_{\mathrm{E}3}(\boldsymbol{x},t) = \frac{-\mathrm{i}}{(2\pi)^3}\int\mathrm{d}^3r\int\mathrm{d}^3m\frac{1}{m_1}\exp\{\mathrm{i}\boldsymbol{m}\cdot(\boldsymbol{x}-\boldsymbol{r})\}\left\{\frac{\partial s_{\mathrm{L}3}(\boldsymbol{r},t)}{\partial r_1}\right.$$

$$\left.+\left[\frac{\partial s_{\mathrm{L}3}(\boldsymbol{r},t)}{\partial r_1}\frac{\partial s_{\mathrm{L}2}(\boldsymbol{r},t)}{\partial r_2}-\frac{\partial s_{\mathrm{L}3}(\boldsymbol{r},t)}{\partial r_2}\frac{\partial s_{\mathrm{L}2}(\boldsymbol{r},t)}{\partial r_1}\right]\right\}\exp\{-\mathrm{i}\boldsymbol{m}\cdot\boldsymbol{s}_{\mathrm{L}}(\boldsymbol{r},t)\}. \quad (3.8)$$

The two space point two time Eulerian correlation function associated with vertical displacement can now be found by using (3.8) to obtain

$$C_{\mathrm{Es}33}(\boldsymbol{X},\tau) = E[s_{\mathrm{E}3}(\boldsymbol{x}+\boldsymbol{X},t+\tau)\,s_{\mathrm{E}3}(\boldsymbol{x},t)]$$

$$= \frac{1}{(2\pi)^3}\int\mathrm{d}^3R\int\mathrm{d}^3m\frac{1}{m_1^2}\exp\{\mathrm{i}\boldsymbol{m}\cdot(\boldsymbol{X}-\boldsymbol{R})\}M_{33}(\boldsymbol{R},\boldsymbol{m},\tau), \quad (3.9)$$

where

$$M_{33}(\boldsymbol{R},\boldsymbol{m},\tau) = E\left[\left\{\frac{\partial s_{\mathrm{L}3}(\boldsymbol{r},t)}{\partial r_1}+\left[\frac{\partial s_{\mathrm{L}3}(\boldsymbol{r},t)}{\partial r_1}\frac{\partial s_{\mathrm{L}2}(\boldsymbol{r},t)}{\partial r_2}-\frac{\partial s_{\mathrm{L}3}(\boldsymbol{r},t)}{\partial r_2}\frac{\partial s_{\mathrm{L}2}(\boldsymbol{r},t)}{\partial r_1}\right]\right\}\right.$$
$$\times\left\{\frac{\partial s_{\mathrm{L}3}(\boldsymbol{r}',t')}{\partial r_1'}+\left[\frac{\partial s_{\mathrm{L}3}(\boldsymbol{r}',t')}{\partial r_1'}\frac{\partial s_{\mathrm{L}2}(\boldsymbol{r}',t')}{\partial r_2'}-\frac{\partial s_{\mathrm{L}3}(\boldsymbol{r}',t')}{\partial r_2'}\frac{\partial s_{\mathrm{L}2}(\boldsymbol{r}',t')}{\partial r_1'}\right]\right\}$$
$$\left.\times\exp\{-\mathrm{i}\boldsymbol{m}\cdot[\boldsymbol{s}_{\mathrm{L}}(\boldsymbol{r},t)-\boldsymbol{s}_{\mathrm{L}}(\boldsymbol{r}',t')]\}\right], \tag{3.10}$$

$\tau = t-t'$, and $\boldsymbol{R} = \boldsymbol{r}-\boldsymbol{r}'$. In obtaining (3.9) we have again used periodic boundary conditions in the vertical as well as the horizontal, used the property (shown in Appendix B) that (3.10) is spatially homogeneous, transformed to the variables $\boldsymbol{R}$ and $\boldsymbol{R}' = \frac{1}{2}(\boldsymbol{r}+\boldsymbol{r}')$, and evaluated the integral over $\boldsymbol{R}'$ to obtain a delta function $\delta(\boldsymbol{m}-\boldsymbol{m}')$ which results in a considerable simplification. Finally, by taking the four-dimensional Fourier transform of (3.9) the four-dimensional Eulerian frequency wavenumber spectrum $S_{\mathrm{Es}33}(\boldsymbol{k},\omega)$ is found to be

$$S_{\mathrm{Es}33}(\boldsymbol{k},\omega) = \int \mathrm{d}^3X \int \mathrm{d}\tau\, C_{\mathrm{Es}33}(\boldsymbol{X},\tau)\exp\{-\mathrm{i}(\boldsymbol{k}\cdot\boldsymbol{X}-\omega\tau)\}$$
$$= \frac{1}{k_1^2}\int \mathrm{d}^3R \int \mathrm{d}\tau\, M_{33}(\boldsymbol{R},\boldsymbol{k},\tau)\exp\{-\mathrm{i}(\boldsymbol{k}\cdot\boldsymbol{R}-\omega\tau)\}. \tag{3.11}$$

The expression for the frequency wavenumber spectrum given by (3.11) is a central result of this paper. Its practical utility, however, depends upon obtaining a tractable expression for the function $M_{33}(\boldsymbol{R},\boldsymbol{k},\tau)$ defined by (3.10). By using the procedure described in Appendix B an exact expression for $M_{33}(\boldsymbol{R},\boldsymbol{k},\tau)$ is obtained. The calculations given in Appendix B are tedious and the final expression for $M_{33}(\boldsymbol{R},\boldsymbol{k},\tau)$ is complicated. Fortunately, it is not necessary to examine all of the details of that result in order to discuss the important features of the Eulerian spectra. The form of the expression for $M_{33}(\boldsymbol{R},\boldsymbol{k},\tau)$ obtained in Appendix B is given by

$$M_{33}(\boldsymbol{R},\boldsymbol{k},\tau) = G_{33}(\boldsymbol{R},\boldsymbol{k},\tau)\exp\left\{-\sum_{\alpha=1}^{3}\sum_{\beta=1}^{3} k_\alpha D_{\alpha\beta}(\boldsymbol{R},\tau)\,k_\beta\right\}, \tag{3.12}$$

where
$$D_{\alpha\beta}(\boldsymbol{R},\tau) = C_{\mathrm{Ls}\alpha\beta}(0,0)-C_{\mathrm{Ls}\alpha\beta}(\boldsymbol{R},\tau), \tag{3.13}$$

and an exact expression for $G_{33}(\boldsymbol{R},\boldsymbol{k},\tau)$ is given. The expression for $G_{33}(\boldsymbol{R},\boldsymbol{k},\tau)$ involves products of spatial derivatives of the Lagrangian correlation functions $C_{\mathrm{Ls}\alpha\beta}(\boldsymbol{R},\tau)$. While this expression is complicated, containing terms which involve products of up to four Lagrangian correlation functions, subsequent calculations, albeit tedious, are tractable. For the most part we shall relegate these calculations to Appendix C and simply discuss the important results in this section.

We note that the exponential factor in (3.12), which is of a Gaussian form in the k_α, plays an important role in determining the wavenumber dependence of the spectrum. For small wavenumbers the Gaussian factor can be expanded in powers of the k_α, while for large wavenumbers an asymptotic expansion in powers of the reciprocals of the k_α is required. It can be shown that the double sum in the exponential factor in (3.12) is positive definite and bounded such that

$$\sum_{\alpha=1}^{3}\sum_{\beta=1}^{3} k_\alpha D_{\alpha\beta}(\boldsymbol{R},\tau)\,k_\beta \leqslant 2\sum_{\alpha=1}^{3} k_\alpha^2 C_{\mathrm{Ls}\alpha\alpha}(0,0) = 2(\nu_{\mathrm{h}}^2 k_{\mathrm{h}}^2+\nu_{\mathrm{v}}^2 k_3^2), \tag{3.14}$$

where
$$\nu_{\mathrm{h}}^2 = C_{\mathrm{Ls11}}(0,0) = C_{\mathrm{Ls22}}(0,0), \tag{3.15}$$

and
$$\nu_{\mathrm{v}}^2 = C_{\mathrm{Ls33}}(0,0). \tag{3.16}$$

The parameters ν_{h} and ν_{v} are the r.m.s. horizontal and vertical Lagrangian displacements which in the second section were referred to as Eulerian lengthscales. Explicit expressions for ν_{h} and ν_{v} are given in Appendix A. If all of the k_α are small enough to assure that the expression given by (3.14) is somewhat less than unity, then the exponential factor in (3.12) can be expanded in powers of the k_α. By using (3.11), (3.12), the lead term in the expression for $G_{33}(\boldsymbol{R},\boldsymbol{k},\tau)$ given in Appendix B, and the above mentioned expansion it can be shown that

$$S_{\mathrm{Es33}}(\boldsymbol{k},\omega) \approx S_{\mathrm{Ls33}}(\boldsymbol{k},\omega). \tag{3.17}$$

We thus find that, for wavenumbers which are small enough to assure that the right-hand side of (3.14) is somewhat less than unity, the Eulerian and Lagrangian frequency wavenumber spectra are approximately equal.

There is a correction to (3.17), also of order k_α^0, which may not be completely negligible. This correction term arises from terms in the expression for $G_{33}(\boldsymbol{R},\boldsymbol{k},\tau)$ which involve products of two Lagrangian correlation functions. This will lead to corrections to the Eulerian frequency wavenumber spectrum given by (3.17) which are in the form of a convolution of two Lagrangian frequency wavenumber spectra, and hence permit frequencies which do not satisfy the dispersion relation. For example, in the calculation of the moored spectra these corrections will lead to non-zero values for the spectrum above the Väisälä cutoff, and thus tend to smear the sharp cutoff at N obtained in the last section. While these correction terms are interesting and perhaps make some important contributions, they are for future investigation and will not be considered further in this paper.

The opposite extreme is the case for which at least one of the k_α is large enough to assure that
$$1 \ll 2(\nu_{\mathrm{h}}^2 k_{\mathrm{h}}^2 + \nu_{\mathrm{v}}^2 k_3^2). \tag{3.18}$$

In this case the exponential factor in (3.12) limits contributions to the integral in (3.11) to come from small values of both $\boldsymbol{R}$ and τ for which the $D_{\alpha\beta}(\boldsymbol{R},\tau)$ are small. In Appendix C an expansion for the Eulerian frequency wavenumber spectrum in powers of the reciprocals of the appropriate large k_α is obtained and it is shown that

$$S_{\mathrm{Es33}}(\boldsymbol{k},\omega) \approx \left(\frac{\pi}{(\eta_{\mathrm{h}}^2 k_{\mathrm{h}}^2 + \eta_{\mathrm{v}}^2 k_3^2)}\right)^{\frac{1}{2}} \exp\left\{\frac{-\omega^2}{4(\eta_{\mathrm{h}}^2 k_{\mathrm{h}}^2 + \eta_{\mathrm{v}}^2 k_3^2)}\right\} \hat{S}_{\mathrm{Es33}}(\boldsymbol{k}), \tag{3.19}$$

where η_{h} and η_{v} are constants whose values are given in Appendix C,

$$\hat{S}_{\mathrm{Es33}}(\boldsymbol{k}) = \frac{1}{2\pi}\int \mathrm{d}\omega\, S_{\mathrm{Es33}}(\boldsymbol{k},\omega) = \frac{1}{k_1^2}\int \mathrm{d}^3R\, M_{33}(\boldsymbol{R},k,0)\exp\{-\mathrm{i}\boldsymbol{k}\cdot\boldsymbol{R}\}, \tag{3.20}$$

and we have used (3.11). Recall that when (3.20) is used in (3.19) at least one of the k_α must be large enough to assure that (3.18) is satisfied. In general the three-dimensional Eulerian wavenumber spectrum given by (3.20) corresponds to the three-dimensional Lagrangian wavenumber spectrum given by (2.17). It is also shown in Appendix C that if (3.18) is satisfied, then

$$\hat{S}_{\mathrm{Es33}}(\boldsymbol{k}) = \frac{1}{k^5}\Psi(\hat{\boldsymbol{k}}), \tag{3.21}$$

where $\hat{\boldsymbol{k}}$ is a unit vector in the direction of $\boldsymbol{k}$. By using (3.21) in (3.19) we find that

if (3.18) is satisfied, then the four-dimensional Eulerian frequency wavenumber spectrum decays as $1/k^6$. Further, unlike the corresponding Lagrangian frequency wavenumber spectrum given by (2.16), the Eulerian frequency wavenumber spectrum is not proportional to the delta functions which confine the system to the dispersion surface. Thus, from an Eulerian frame point of view, at large wavenumbers the dispersion surface is completely smeared and the system is not wavelike.

We have found that at small wavenumbers, for which the inequality in (3.18) is reversed, the Eulerian and Lagrangian frequency wavenumber spectra are approximately equal. At larger wavenumbers, for which (3.18) is satisfied, the Eulerian frequency wavenumber spectrum decays as $1/k^6$, while the Lagrangian frequency wavenumber spectrum decays as the convergence factor $h(\boldsymbol{k})$. We note that both (3.19) and (3.21) are independent of the detailed nature of $h(\boldsymbol{k})$. Thus, while the Lagrangian spectra (see (2.16) and (2.17)) are directly sensitive to the details of $h(\boldsymbol{k})$, the corresponding Eulerian spectra are not.

Some of the one-dimensional marginal spectra, such as the frequency spectra and moored coherences discussed in the last section, are obtained by integrating over all wavenumbers. In the case of both Lagrangian and Eulerian spectra such integrals are dominated by contributions from small k_α where the Eulerian and Lagrangian frequency wavenumber spectra are approximately equal. In the case of Eulerian spectra the $1/k^6$ decay simply provides a large wavenumber cutoff at approximately the surface defined by

$$(\nu_{\mathrm{h}}^2 k_{\mathrm{h}}^2 + \nu_{\mathrm{v}}^2 k_3^2) = 1. \tag{3.22}$$

In the case of Lagrangian spectra the Lagrangian convergence factor $h(\boldsymbol{k})$ provides a large wavenumber cutoff at approximately the surface defined by

$$(\mu_{\mathrm{h}}^2 k_{\mathrm{h}}^2 + \mu_{\mathrm{v}}^2 k_3^2) = 1. \tag{3.23}$$

For both case I and case II $\nu_{\mathrm{h}} < \mu_{\mathrm{h}}$ and $\nu_{\mathrm{v}} < \mu_{\mathrm{v}}$ so that the Lagrangian convergence factor controls the cutoff for both Lagrangian and Eulerian spectra. For case III it will be shown in the next section that $\nu_{\mathrm{h}} \approx \mu_{\mathrm{h}}$ and $\nu_{\mathrm{v}} \approx \mu_{\mathrm{v}}$ so that the surfaces defined by (3.22) and (3.23) are approximately the same. Hence, for all of the above three cases the one-dimensional Eulerian frequency spectra and coherences are approximately equal to the corresponding Lagrangian spectra.

The horizontal tow spectrum, on the other hand, is an Eulerian spectrum and presents a different situation. It can be obtained from the three-dimensional wavenumber spectrum given by (3.20) by setting $k_1 = \kappa$ and integrating over k_2 and k_3. For small κ such that the product $\kappa\nu_{\mathrm{h}}$ is somewhat less than unity the integrals are dominated by small values of k_2 and k_3 so that the Eulerian tow spectrum is approximately equal to the one-dimensional Lagrangian horizontal wavenumber spectrum. The one-dimensional Lagrangian wavenumber or tow spectrum $\mathrm{HTS}_{\mathrm{Ls33}}(\kappa)$ is found by using (2.17) and (2.38) to write

$$\begin{aligned}\mathrm{HTS}_{\mathrm{Es33}}(\kappa) \approx \mathrm{HTS}_{\mathrm{Ls33}}(\kappa) &= \frac{1}{(2\pi)^2}\int \mathrm{d}k_2 \int \mathrm{d}k_3\, \hat{S}_{\mathrm{Ls33}}(k_1 = \kappa, k_2, k_3) \\ &= \frac{E_0}{(2\pi)^2 \rho}\int \mathrm{d}k_2 \int \mathrm{d}k_3 \frac{(\kappa^2 + k_2^2)\exp\{-\frac{1}{2}[\mu_{\mathrm{h}}^2 k_2^2 + \mu_{\mathrm{v}}^2 k_3^2]\}}{[N^2(\kappa^2 + k_2^2) + f^2 k_3^2]}.\end{aligned} \tag{3.24}$$

The spectrum given by (3.24) is white for small κ and transitions to a Gaussian decay at large κ. This Gaussian decay is completely due to the form of $h(\boldsymbol{k})$ and is not

meaningful. The white spectrum at small κ is of interest and the level is found by evaluating (3.24) at $\lambda = 0$ to obtain

$$\mathrm{HTS}_{\mathrm{Es33}}(\kappa = 0) \approx \mathrm{HTS}_{\mathrm{Ls33}}(\kappa = 0) = \frac{E_0}{2\pi\rho\mu_{\mathrm{h}}^2 Nf(1+N\mu_{\mathrm{v}}/f\mu_{\mathrm{h}})}. \tag{3.25}$$

For larger κ such that the product $\kappa\nu_{\mathrm{h}}$ is somewhat larger than unity the expression given by (3.21) is appropriate and a significantly different result is obtained. By setting $k_1 = \kappa$, $k_2 = \kappa\xi_2$, and $k_3 = \kappa\xi_3$ and by using (3.21) it is straightforward to show that

$$\mathrm{HTS}_{\mathrm{Es33}}(\kappa) = \frac{1}{(2\pi)^2}\int \mathrm{d}k_2 \int \mathrm{d}k_2 \hat{S}_{\mathrm{Es33}}(k_1 = \kappa, k_2, k_3) = \frac{W}{\kappa^3}, \tag{3.26}$$

where an expression for W which depends upon N, f, E_0, μ_{h}, and μ_{v} is given in Appendix C. We have thus found that the one-dimensional Eulerian horizontal tow spectrum is white at small κ and transitions to a κ^{-3} at large κ. In the fourth section we shall present a comparison of these results to experiment and show that the agreement is excellent.

As a final example of Eulerian tow spectra, we now consider the vertical tow or drop spectrum $\mathrm{VTS}_{\mathrm{Es33}}(\iota)$. This spectrum is found from (3.20) by setting $k_3 = \iota$ and integrating over k_1 and k_2. Again we find that if ι is small such that $\iota\nu_{\mathrm{v}}$ is somewhat less than unity, then the Eulerian and Lagrangian spectra are approximately equal. In this case we can use (2.17) and (2.38) to write

$$\begin{aligned}\mathrm{VTS}_{\mathrm{Es33}}(\iota) \approx \mathrm{VTS}_{\mathrm{Ls33}}(\iota) &= \frac{1}{(2\pi)^2}\int \mathrm{d}k_1 \int \mathrm{d}k_2 \hat{S}_{\mathrm{Ls33}}(k_1, k_2, k_3 = \iota) \\ &= \frac{E_0}{2\pi\rho}\int_0^\infty \mathrm{d}k_{\mathrm{h}} \frac{k_{\mathrm{h}}^3 \exp\{-\frac{1}{2}[\mu_{\mathrm{h}}^2 k_{\mathrm{h}}^2 + \mu_{\mathrm{v}}^2 \iota^2]\}}{[N^2 k_{\mathrm{h}}^2 + f^2\iota^2]}.\end{aligned} \tag{3.27}$$

It is only small values of ι for which (3.27) is appropriate and there the spectrum is white at the level

$$\mathrm{VTS}_{\mathrm{Es33}}(\iota = 0) \approx \mathrm{VTS}_{\mathrm{Ls33}}(\iota = 0) = \frac{E_0}{2\pi\rho N^2 \mu_{\mathrm{h}}^2}. \tag{3.28}$$

It is shown in Appendix C that if the product $\iota\nu_{\mathrm{v}}$ is somewhat larger than unity, then

$$\mathrm{VTS}_{\mathrm{Es33}}(\iota) = \frac{1}{(2\pi)^2}\int \mathrm{d}k_1 \int \mathrm{d}k_2 \hat{S}_{\mathrm{Es33}}(k_1, k_2, k_3 = \iota) = \frac{\overline{W}}{\iota^3}, \tag{3.29}$$

where an expression for $\overline{W}$ which depends upon N, f, E_0, μ_{h}, and μ_{v} is also given in Appendix C. We have thus found that the vertical Eulerian tow spectrum is white at small ι and transitions to an ι^{-3} decay at large ι. In the fourth section these results are compared to experiment and excellent qualitative agreement is obtained.

4. Discussion

We have obtained expressions for the four-dimensional Eulerian frequency wavenumber spectra which are given in terms of the various four-dimensional Lagrangian frequency wavenumber spectra (we have illustrated this for vertical displacement but it is clear that any other of the various Eulerian spectra can also be obtained). These expressions establish a clear relationship between the observed

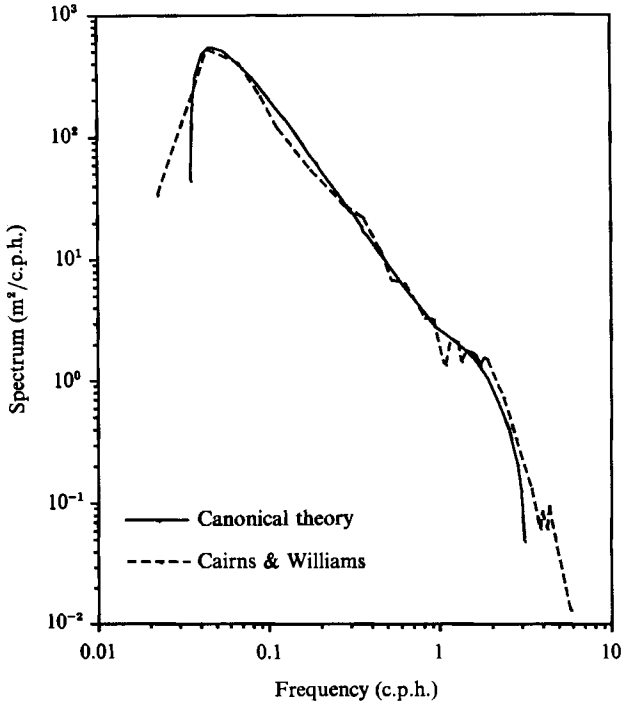

FIGURE 1. A comparison between the results of the canonical theory and experiment for a typical moored vertical displacement spectrum.

Eulerian spectra and the fundamental Lagrangian quantities usually studied in statistical mechanics. At small wavenumbers the Eulerian and Lagrangian spectra are approximately equal, but at large wavenumbers they are significantly different. We now turn to a comparison of our theoretical results to experiment.

We shall first consider the case of the moored spectra which will be compared to the Lagrangian frequency spectra and coherencies computed in §2. While the measured spectra in some experiments are in terms of Lagrangian variables and in other experiments in terms of Eulerian variables, we have shown that for moored measurements the two types of spectra are approximately equal. Thus, the following comparison is appropriate regardless of the type of measurement being considered. We emphasize that for now we are only seeking to establish general qualitative agreement. In the following comparison the values of N and f are chosen to correspond to the particular experiment under consideration and we will simply adjust the parameters E_0, μ_h, and μ_v in order to obtain a reasonable comparison. We will show later that the assumed values for these parameters are consistent with the scenario referred to as case III. In figure 1 the solid curve is a plot of the moored vertical displacement spectrum given by (2.42) where for the purpose of this plot we have chosen $E_0/\rho = 1.2 \times 10^5$ J m^3/kg, $\mu_h = 700$ m, $\mu_v = 7$ m, $r_3 = 350$ m, $N = 3.2$ c.p.h., and $f = 0.035$ c.p.h. The dashed curve in figure 1 is a reproduction of a curve given by Cairns & Williams (1976). The Cairns & Williams result corresponds to a moored experiment conducted at a depth of approximately 350 m in a location approximately 800 km off shore of San Diego, California and is typical of moored experiments. The excellent qualitative agreement is obvious.

In figure 2 the solid curve is a plot of the moored vertical velocity spectrum given

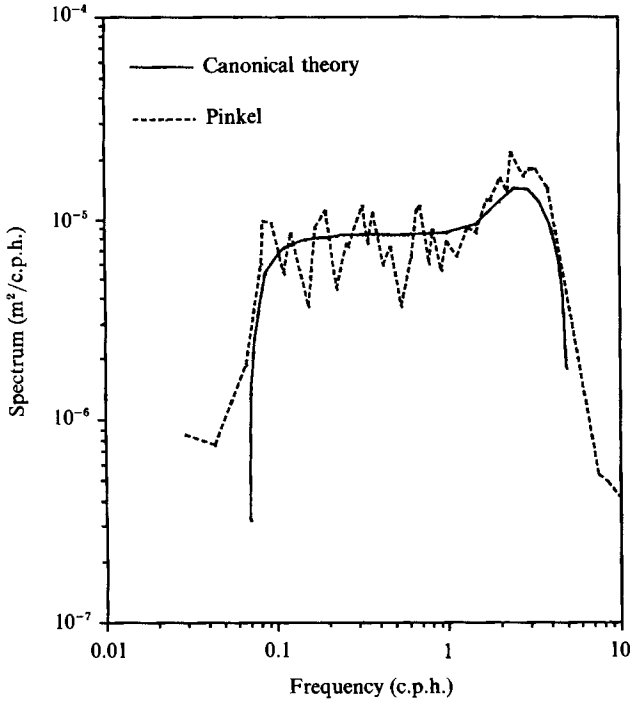

FIGURE 2. A comparison between the results of the canonical theory and experiment for a typical moored vertical velocity spectrum.

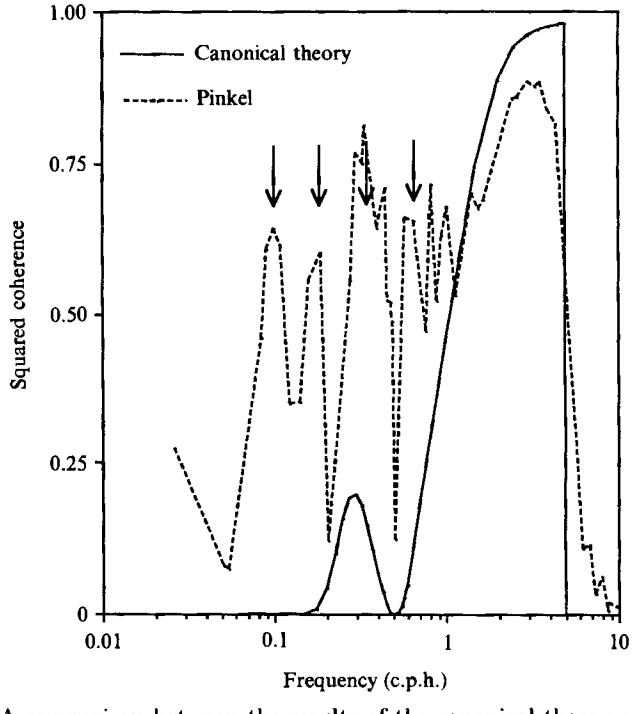

FIGURE 3. A comparison between the results of the canonical theory and experiment for a typical example of moored vertical coherence.

by (2.44) where for the purpose of this plot we have chosen $E_0/\mu = 4.2 \times 10^4$ J m^3/kg, $\mu_h = 400$ m, $\mu_v = 4$ m, $r_3 = 200$ m, $N = 5.0$ c.p.h., and $f = 0.070$ c.p.h. The dashed curve in figure 2 is a reproduction (which includes a change in length units from cm to m) of a curve given by Pinkel (1981). The Pinkel result corresponds to a moored experiment conducted at a depth of approximately 200 m, and is also typical of moored measurements. The excellent qualitative agreement is again obvious. In figure 3 the solid curve is a plot of the moored vertical coherence given by (2.45) where the vertical separation is 40 m and the other parameters are the same as in figure 2. The dashed curve in figure 3 is also a reproduction of a curve given by Pinkel (1981) for which the vertical separation was 36 m. The four vertical arrows in figure 3 indicate the frequencies of the semidiurnal tide and its first three harmonics so that there seems to be considerable tidal contamination at the lower frequencies. Again the excellent qualitative agreement is apparent.

There are a number of other moored spectra and coherences, such as the moored horizontal velocity autospectrum and the moored horizontal coherence, which are easily computed but we shall not present these results here. The calculations are entirely similar to the above and the results are in equally good agreement with experiment. We emphasize again that we are only seeking to establish general qualitative agreement. However, we would like to demonstrate that the values chosen for the various parameters are at least reasonable. While the two sets of values for the parameters E_0, μ_h, and μ_v are not identical, they are certainly similar. For example, the values for the overall energy scaling parameter E_0 are well within the range of variability observed in experiments. The lengthscales μ_h and μ_v are used in conjunction with wavenumbers (i.e. are in radian measure) and, therefore, correspond to wavelengths which are greater by the factor 2π. Since we have used the constant N model for the vertical eigenfunctions, some distortion of vertical distances is likely and the above values should be taken only as rough estimates. Nevertheless, the above lengthscales are roughly the same as those for which Holloway (1980, 1982) argues that the weak interaction approximation breaks down. Further, it is shown in Appendix A that the values for these lengthscales as well as the overall scale factor E_0 are consistent with the scenario referred to as case III. This issue will be discussed in greater detail later in this section.

We shall now consider some examples of tow spectra. The tow spectra are always Eulerian and mostly at wavenumbers for which the Eulerian and Lagrangian spectra are different. The first example we will discuss is the horizontal tow spectrum $\mathrm{HTS}_{\mathrm{Es}33}(\kappa)$ which was found at large wavenumbers to decay as κ^{-3}. This decay is similar to that which is observed experimentally and is independent of the detailed nature of the Lagrangian convergence factor. The solid curve in figure 4 is a plot of the horizontal two spectrum given by (3.26) and (C32) where for the purpose of this plot we have chosen $E_0/\rho = 1.4 \times 10^5$ J m^3/kg, $\mu_h = 700$ m, $\mu_v = 7$ m, $N = 2.5$ c.p.h., and $f = 0.035$ c.p.h. The dashed curve is the $\kappa = 0$ limit of the Lagrangian horizontal tow spectrum given by (2.35), which is approximately the level of the Eulerian horizontal tow spectrum at small κ. The points plotted as a scattergram in figure 4 are reproduced from an experimental result given by Katz (1975). The Katz result corresponds to a towed experiment conducted in the Sargasso Sea at a depth between 700 and 800 m. This result is typical of towed measurements. While the agreement between our theoretical result and experiment is not perfect, the qualitative similarity between the two is apparent. We have not computed the theoretical Eulerian spectrum for wavelengths between 1 km and 10 km because this is not in either asymptotic region and would require a numerical integration. It is clear,

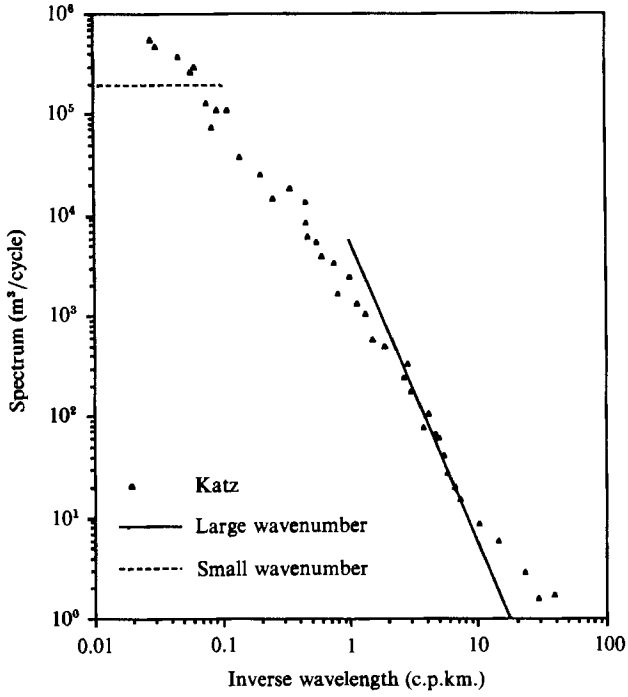

FIGURE 4. A comparison between the results of the canonical theory and experiment for a typical vertical displacement horizontal tow spectrum.

however, that near 1 km the curve breaks to a smaller slope and finally merges with the dashed curve at approximately 10 km. There is a noticeable difference between our theory and experiment at very small wavenumbers (i.e. near the dotted curve in figure 4) where the Lagrangian and Eulerian spectra are approximately equal. This difference may indicate a departure from canonical equilibrium at small wavenumbers. Such a departure would not be surprising, since it is at these small wavenumbers where source contributions are thought to be strong. We should also point out that our theoretical tow spectrum assumes an infinite tow speed, while in the Katz experiment the actual tow speed was only about 2.5 m/s. At wavelengths greater than a few km finite tow-speed effects can be significant and may be contributing to the Katz result at the longer wavelengths. Also, our treatment does not include the translational or geostrophic modes which may contribute significantly to the measured result.

As a final example of an Eulerian tow spectrum we now consider the vertical tow or drop spectrum $\mathrm{VTS}_{\mathrm{Es33}}(\iota)$. If the product $\iota\nu_{\mathrm{v}}$ is somewhat less than unity, then the Eulerian vertical tow spectrum is approximately equal to the Lagrangian vertical tow spectrum which, at small wavenumbers, is white at the level given by (3.28). If the product $\iota\nu_{\mathrm{v}}$ is somewhat larger than unity, then the spectrum decays as ι^{-3} and is given by (3.29). The solid curve in figure 5 is a plot of the vertical tow spectrum given by (3.29) and (C34) where for the purpose of this plot we have chosen $E_0/\rho = 1.4 \times 10^5$ J m^3/kg, $\mu_{\mathrm{h}} = 930$ m, $\mu_{\mathrm{v}} = 9.3$ m, $N = 3.0$ c.p.h., and $f = 0.042$ c.p.h. The dashed curve is the $\iota = 0$ limit of the Lagrangian vertical tow spectrum given by (3.28), which is approximately the level of the Eulerian vertical tow spectrum at small ι. We have not computed the theoretical spectrum at inverse wavelengths

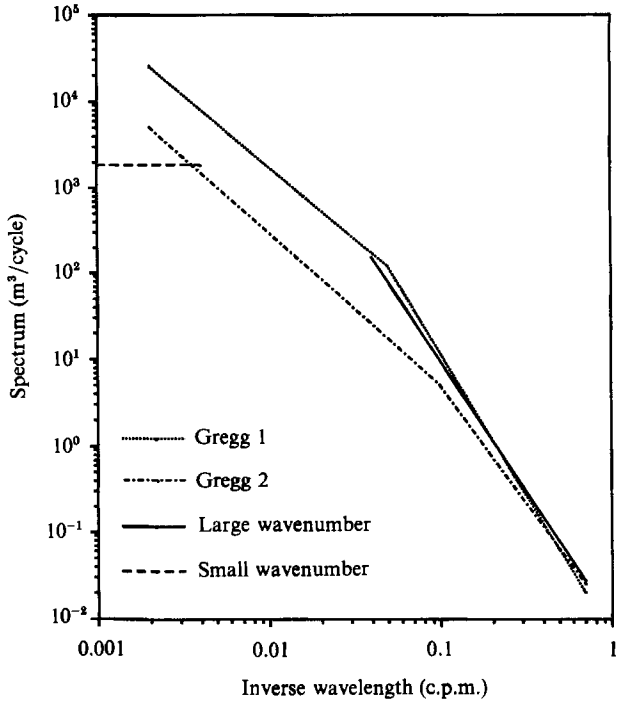

FIGURE 5. A comparison between the results of the canonical theory and experiment for a typical vertical displacement vertical tow spectrum.

between 0.004 c.p.m. and 0.04 c.p.m. because this would require numerical integration. It is clear, however, that below 0.04 c.p.h. the curve breaks to a smaller slope and finally merges with the dashed curve at approximately 0.004 c.p.m. The dotted curve and the dash–dot curve are typical examples of measured vertical tow spectra which we have reproduced from results given by Gregg (1977). The curves given by Gregg are actually regression fits to two experiments which have been chosen for comparison simply because they are representative and were easy for us to reproduce. Again the agreement between the canonical theory and experiment is apparent. While there is some disagreement at very small wavenumbers, considering the simplicity of our model (i.e. infinite drop speed, constant N, periodic boundary conditions in the vertical, etc.) we believe that the comparison is quite favourable.

For all of the results we have presented here the values of N and f were those which were appropriate for the particular experiment under consideration. The parameters E_0, μ_h, and μ_v were adjusted to obtain reasonable agreement with experiment. While these parameters were adjusted, the resulting values are all consistent with each other and it is clear that we could have chosen a single set of parameters and obtained fair agreement with all of the data sets. Considering the simplicity of our model, the degree of agreement we have obtained here is striking. We have thus demonstrated that the assumption that the oceanic internal wave system is near canonical equilibrium can yield expressions for various marginal spectra associated with both moored and towed measurements which are in excellent qualitative agreement with experiment. In order to accomplish this it was important to consider the role played by strong dynamic nonlinear interactions in limiting the participation of those modes which correspond to small lengthscales. It was also important to distinguish

Parameter	Cairns & Williams	Pinkel	Katz	Gregg
E_0/ρ (J m^3/kg)	1.2×10^5	4.2×10^4	1.4×10^5	1.4×10^5
μ_h (m)	7.0×10^2	4.0×10^2	7.0×10^2	9.3×10^2
μ_v (m)	7.0	4.0	7.0	9.3
λ	1.1	2.7	2.1	0.4
ν_h (m)	2.1×10^2	5.3×10^2	4.8×10^2	1.6×10^2
ν_v (m)	3.8	9.5	8.6	2.8

TABLE 1. Values of the various parameters used in the comparison between theory and experiment and the values obtained for the nonlinear energy parameter λ

carefully between Lagrangian and Eulerian variables. It was necessary, therefore, to go beyond the simple treatment which equipartitions energy among all of the internal wave modes and considers only Lagrangian quantities.

We have considered three distinct cases for which the phase-space density function has the Gaussian form given by (2.7). In all three cases expectation values of Eulerian quantities which are obtained from the corresponding Lagrangian quantities by using the transformation (3.1) can be computed exactly. The scenario referred to as case I is, in fact, just the above simple treatment. It is clear that case I is not adequate to describe the oceanic observations. We have included it here for completeness since it is the case usually associated with canonical equilibrium. The scenario referred to as case II is the one that is usually considered to be appropriate for the oceanic internal wave system. There are, however, several difficulties associated with this case which were discussed in §2. The scenario referred to as case III is the one which we propose may eventually provide a first-principles explanation for the experimental observations.

In principle it should be possible to compute the lengthscales μ_h and μ_v from a detailed knowledge of the nonlinear interactions once the level E_0 has been specified. Such an investigation is important for a full understanding of the physics, but it is beyond the scope of our considerations in this paper. It has not been our intent to present this work as complete. Rather, we have sought only to present enough evidence to support a reasonable argument in favour of case III and more importantly to elucidate the differences between Lagrangian and Eulerian spectra. Many important, and we believe fruitful, investigations remain to be done. However, it is important for us to demonstrate now that the various values we have chosen for the parameters are consistent among themselves and with the basic tenets of case III. In table 1 the various values of the parameters E_0/ρ, μ_h, and μ_v which were used in our comparisons to experiment are given. From the table it can be seen that all of the values are within a factor of 3.5 from each other, and if we neglect the Pinkel result, which was nearer the surface than the others, then the variation is even smaller. We should point out that in adjusting the above parameters we have fixed the ratio μ_h/μ_v at 100. There was no particular reason for this choice other than convenience and it seems to work well. Certainly some adjustment of this ratio is possible. In fact, in view of the simple constant N model we have used, all of the above values should be considered only rough estimates.

In table 1 we also present the values of a nonlinear energy parameter λ for each of the experiments, where for convenience we have set the parameter $c = (\mu_h f/\mu_v N)^2 - 1$ (defined in Appendix A) equal to unity. The nonlinear energy

parameter λ, which is defined and computed in Appendix A, should be of order unity if case III is to be considered reasonable. The parameter λ is a relative measure of the strength of the nonlinear interactions which, if it is much larger than unity, indicates that the nonlinear interactions are too large for the weak interaction approximation to be considered valid. On the other hand, if λ is much less than unity, then the nonlinear interactions are too small to provide the required large-wavenumber cutoff. As can be seen from the table all of the values for λ are of order unity. We also note that all of these considerations are entirely consistent with the arguments given by Holloway (1980, 1982) concerning the breakdown of the weak interaction approximation.

Finally, in table 1 we give the values of the Eulerian lengthscales ν_h and ν_v, where again we have set the parameter c equal to unity. All of the values are within a factor of 2.5 of each other and are, therefore, consistent among themselves. We note that the Eulerian lengthscales are of the same order of magnitude as the corresponding Lagrangian lengthscales and this is consistent with case III. This also means that Eulerian tow measurements cannot reveal the details of the Lagrangian convergence factor $h(\boldsymbol{k})$. The transition into the Eulerian decay (i.e. κ^{-3} or ι^{-3} for the one-dimensional tow spectra) occurs at approximately the same value for the wavenumber as does the transition into the decaying part of the Lagrangian convergence factor and, thus, masks the details of $h(\boldsymbol{k})$. We emphasize again that the above values should be taken as rough estimates, and that in this paper we are only trying to establish reasonable consistency.

In our earliest consideration of these methods (Allen & Joseph 1988) we had not fully appreciated the role of the nonlinear interactions in establishing the Eulerian lengthscales ν_h and ν_v, and considered the case for which the Eulerian lengthscales were much larger than the corresponding Lagrangian lengthscales. It is now clear that this was not a physically meaningful case. Thus, some of the detailed results presented in that paper are not physically meaningful, but the basic concept and the general methods are the same as here and remain valid. It is clear that a more detailed investigation of the role of strong nonlinear interactions within the Lagrangian frame is needed. As pointed out earlier, it should be possible to compute the Lagrangian lengthscales μ_h and μ_v from a detailed knowledge of the nonlinear interactions, and this would then establish a precise condition for the strength of the nonlinear interactions. This is an important subject for future investigation.

While our comparison to experiment has tended to emphasize canonical equilibrium via case III, the more important result is our relation between Eulerian and Lagrangian spectra and the demonstration that the two can be significantly different. None of the marginal Eulerian spectra which are usually measured are very sensitive to the details of the underlying Lagrangian spectra. Thus, it is possible that the Lagrangian spectra differ considerably from canonical equilibrium and still result in Eulerian spectra which are entirely similar to those obtained from case III. It is important to realize that the fundamental dynamical processes directly impact the Lagrangian spectra but are masked in the Eulerian spectra by the advective tail. Experiments which obtain Lagrangian information are required in order to study these fundamental dynamical processes. For example, dye measurements with coded dye, or in conjunction with vertical temperature measurements, or perhaps some type of card experiment (Munk, private communication) would be useful for determining the decaying part of the Lagrangian wavenumber spectrum. Other possible experiments might be suggested, but it is clear that some measurement which explores this issue is needed.

Another interesting and potentially important result is that the four-dimensional Eulerian frequency wavenumber spectrum is not confined to the dispersion surface. So far as we are aware no experimental evidence concerning this issue exists. The Doppler sonar observations of Pinkel (1984) are a step in this direction, but so far have been able to yield only two-dimensional frequency wavenumber spectra. Since the two-dimensional spectra are obtained by integrating over two components of the three-dimensional wavevector, information concerning the existence of delta functions (i.e. sharp peaks) which confine the system to the dispersion surface is lost. Our expressions can be used to compute theoretical expressions to be compared with Pinkel's results. While such a comparison would certainly be interesting and the calculations are tractable, they are also non-trivial and have yet to be completed.

In this paper, as previously noted, we have neglected the translational modes. By so doing we have ignored possible alterations to the spectra in regions with substantial mean currents as well as some potentially important issues concerning diffusion. The methods we have introduced here are also capable of including the translational modes and thus can be considered for a variety of additional investigations. This is another potentially important area for future research.

As a final point we note that the eikonal technique which is discussed by Henyey & Pomphrey (1983) is also a method for describing the effects of the advective nonlinearity. Subsequently Flatté, Henyey & Wright (1985) have used the eikonal technique in a numerical Monte-Carlo study to show that at small scales an initial distribution of test wave packets evolves to the GM distribution. They argue that the eikonal technique avoids the weak interaction approximation and can be used to treat strong nonlinear interactions. However, it is important to realize that their treatment is in terms of Eulerian variables and includes only contributions from the advective nonlinearity. They completely neglect contributions from the dynamic nonlinearities, and for that case our use of the weak interaction approximation in the canonical theory, since the dynamics is in terms of Lagrangian variables, is exact. Their results from the eikonal technique and ours from the canonical theory both seem to imply that the observed distribution of small-scale internal waves is a consequence of advection. In this sense the two methods seem to complement each other. On the other hand, there are differences between the two methods which need to be understood. The canonical theory treats the Lagrangian excitations as waves while the eikonal technique treats the Eulerian excitations as waves. The canonical theory includes the statistics as an integral part of the theory, while the eikonal technique treats the statistics by the use of Monte-Carlo methods. The canonical theory predicts Eulerian spectra which exhibit non-wavelike properties at small lengthscales. so far as we are aware, the Monte-Carlo methods have not been used to generate a four-dimensional frequency wavenumber spectrum which might reveal non-wavelike behaviour. Our method can also be used to study the statistics of the time evolution of an initial wavepacket in the presence of a random internal wave background. This corresponds to the problem studied by using the eikonal technique and we suspect that a comparison of the two methods would reveal some differences. In any case the relation between the two methods needs clarification.

We have now established that case III is consistent with the experimental observations. We have not ruled out, however, that case II may still be the appropriate description for oceanic internal waves. On the other hand, if case II is the appropriate description, then $h(\boldsymbol{k})$ is determined by some external heat bath but the Eulerian lengthscales ν_{h} and ν_{v} are the same as in case III. This is because the Eulerian lengthscales can be obtained from the area under the corresponding moored

frequency spectrum, which can be determined experimentally and are independent of whether case II or case III is the appropriate description. In either case most of the observed tow spectrum is at wavenumbers which are in the advective Eulerian tail. While it is possible that case II is the appropriate description, we believe that case III offers the more attractive possibilities.

This research was supported in part by the Office of Naval Research Contract N00024-95-C-5301 and in part by a J. H. Fitzgerald Dunning Professorship (K. R. A.) at the Department of Electrical and Computer Engineering of The Johns Hopkins University awarded by The Johns Hopkins University/Applied Physics Laboratory. The authors would like to thank Professor O. M. Phillips for carefully reading the original manuscript and making many useful suggestions, and Drs J. R. Apel and L. W. Hart for helpful discussions.

Appendix A. Some important Lagrangian quantities

In this Appendix we compute a number of Lagrangian quantities which are used throughout the paper. We first compute the Eulerian lengthscales ν_h and ν_v. By using (1.18), (2.7) and (2.14) it is straightforward to show that

$$\nu_h^2 = C_{Ls11}(0,0) = \frac{E_0}{(2\pi)^3\rho}\int d^3l \frac{h(l)\,l_3^2}{\Omega^2(l)\,l^2 l_h^2}\left[l_1^2 + \frac{f^2 l_2^2}{\Omega^2(l)}\right]. \tag{A 1}$$

By using (2.3), (2.38), working in cylindrical coordinates, setting $l_3 = l_h y$, and evaluating the horizontal integrations (A 1) reduces to

$$\nu_h^2 = \frac{E_0 a^2}{4(2\pi^3)^{\frac{1}{2}}\rho N^2 \mu_h^2 \mu_v}\int_0^1 dx \frac{x^2}{[1+cx^2]}\left[1 + \frac{b^2[1+(a^2-1)\,x^2)]}{[1+cx^2]}\right], \tag{A 2}$$

where

$$a = \frac{\mu_h}{\mu_v}, \quad b = \frac{f}{N}, \quad c = a^2 b^2 - 1. \tag{A 3}$$

By using the same procedure it is straightforward to show that

$$\nu_v^2 = C_{Ls33}(0,0) = \frac{E_0}{2(2\pi^3)^{\frac{1}{2}}\rho N^2 \mu_h^2 \mu_v}\int_0^1 dx \frac{(1-x^2)}{[1+cx^2]}. \tag{A 4}$$

Finally (A 2) and (A 4) can be written

$$\nu_h^2 = \frac{E_0 a^2}{4(2\pi^3)^{\frac{1}{2}}\rho N^2 \mu_h^2 \mu_v}[A_2 + b^2 A_3 + b^2(a^2-1)\,A_4], \tag{A 5}$$

and

$$\nu_v^2 = \frac{E_0}{2(2\pi^3)^{\frac{1}{2}}\rho N^2 \mu_h^2 \mu_v}[A_1 - A_2], \tag{A 6}$$

where

$$A_1 = \int_0^1 dx \frac{1}{[1+cx^2]} = \frac{1}{c^{\frac{1}{2}}}\tan^{-1} c^{\frac{1}{2}}, \tag{A 7}$$

$$A_2 = \int_0^1 dx \frac{x^2}{[1+cx^2]} = \frac{1}{c}\left[1 - \frac{1}{c^{\frac{1}{2}}}\tan^{-1} c^{\frac{1}{2}}\right], \tag{A 8}$$

$$A_3 = \int_0^1 dx \frac{x^2}{[1+cx^2]^2} = \frac{1}{2c}\left[\frac{1}{c^{\frac{1}{2}}}\tan^{-1} c^{\frac{1}{2}} - \frac{1}{1+c}\right], \tag{A 9}$$

and
$$A_4 = \int_0^1 dx \frac{x^4}{[1+cx^2]^2} = \frac{1}{2c^2}\left[\frac{3+2c}{1+c} - \frac{3}{c^{\frac{1}{2}}}\tan^{-1} c^{\frac{1}{2}}\right]. \tag{A 10}$$

We now obtain an estimate of the strength of the nonlinear interactions. It is sufficient for our purposes here to consider the first contributing nonlinear term from the Jacobian determinant. If we define $s_{\alpha\beta}$ such that

$$s_{\alpha\beta} = \frac{\partial s_{L\alpha}}{\partial r_\beta}, \tag{A 11}$$

then the Jacobian determinant J can be written as

$$\begin{aligned} J &= 1 + [s_{11} + s_{22} + s_{33}] + [(s_{11}s_{33} - s_{13}s_{31}) + (s_{22}s_{33} - s_{23}s_{32}) + (s_{11}s_{22} - s_{12}s_{21})] \\ &\quad + [s_{13}(s_{21}s_{32} - s_{22}s_{31}) + s_{23}(s_{12}s_{31} - s_{11}s_{32}) + s_{33}(s_{11}s_{22} - s_{12}s_{21})] \\ &= 1 + F_1 + F_2 + F_3, \end{aligned} \tag{A 12}$$

where the F_n, $1 \leqslant n \leqslant 3$, correspond respectively to the terms in square brackets. We note that F_1, which is linear in the displacements, is the divergence of the displacement and in our non-compressional approximation is zero. The first contributing nonlinear term is F_2 which is quadratic in the displacements.

In our treatment of the compressional potential energy we expanded $1/J^{\gamma-1}$ about the point $J = 1$, and if that expansion is to be valid then the contributions from the F_n must be small relative to unity. We can estimate the strength of the nonlinear interactions by computing the expectation values of the F_n. By using (2.7), (2.14) and (A 12) it is easy to show that $E[F_2] = E[F_3] = 0$ so that the lowest-order contributing term is described by $E[F_2^2]$. We therefore define the nonlinear energy parameter λ such that

$$\lambda^2 = E[F_2^2]. \tag{A 13}$$

If λ is of order unity, then the expansion is in the process of breaking down. A precise statement of this condition requires a more detailed study, but the above is adequate for our purposes here.

From (A 12) it can be seen that F_2^2 consists of a number of terms which are quartic in the displacements. For the Gaussian distribution given by (2.7) the expectation value of a quartic term can be written as products of expectation values of pairs of displacements. It is tedious but straightforward to show that the following expectation values are required for this calculation:

$$E[s_{11}^2] = E[s_{22}^2] = BI_1, \tag{A 14}$$

$$E[s_{33}^2] = -2E[s_{11}s_{33}] = -2E[s_{13}s_{31}] = -2E[s_{22}s_{33}] = -2E[s_{23}s_{32}] = 2BI_2, \tag{A 15}$$

$$E[s_{13}^2] = -2E[s_{23}^2] = Ba^2I_3, \tag{A 16}$$

$$E[s_{31}^2] = -2E[s_{32}^2] = B\frac{1}{a^2}I_4, \tag{A 17}$$

$$E[s_{11}s_{22}] = -2E[s_{12}s_{21}] = BI_5, \tag{A 18}$$

$$E[s_{12}^2] = -2E[s_{21}^2] = BI_6, \tag{A 19}$$

where the common scale factor B is given by

$$B = \frac{3E_0}{4(2\pi^3)^{\frac{1}{2}}\rho N^2 \mu_{\mathrm{h}}^2 \mu_{\mathrm{v}}^3} \tag{A 20}$$

and $I_1 - I_6$ are given by the integrals

$$I_1 = \frac{1}{4}\int_0^1 \mathrm{d}x \frac{x^2(1-x^2)}{[1+cx^2]}\left[3+\frac{b^2[1+(a^2-1)x^2]}{[1+cx^2]}\right], \tag{A 21}$$

$$I_2 = \int_0^1 \mathrm{d}x \frac{x^2(1-x^2)}{[1+cx^2]}, \tag{A 22}$$

$$I_3 = \int_0^1 \mathrm{d}x \frac{x^4}{[1+cx^2]}\left[1+\frac{b^2[1+(a^2-1)x^2]}{[1+cx^2]}\right], \tag{A 23}$$

$$I_4 = \int_0^1 \mathrm{d}x \frac{(1-x^2)^2}{[1+cx^2]}, \tag{A 24}$$

$$I_5 = \frac{1}{4}\int_0^1 \mathrm{d}x \frac{x^2(1-x^2)}{[1+cx^2]}\left[1-\frac{b^2[1+(a^2-1)x^2]}{[1+cx^2]}\right], \tag{A 25}$$

and

$$I_6 = \frac{1}{4}\int_0^1 \mathrm{d}x \frac{x^2(1-x^2)}{[1+cx^2]}\left[1+\frac{3b^2[1+(a^2-1)x^2]}{[1+cx^2]}\right]. \tag{A 26}$$

It is then straightforward to show that

$$\lambda = B[5I_2^2 + 2I_3 I_4 + 2I_1 I_2 + I_1^2 + 2I_5^2 + I_6^2]^{\frac{1}{2}}. \tag{A 27}$$

Finally, the integrals I_1–I_6 can be written in terms of the four basic integrals

$$\hat{I}_1 = \int_0^1 \mathrm{d}x \frac{x^2(1-x^2)}{[1+cx^2]} = \left(\frac{1+c}{c}\right)A_2 - \frac{1}{3c}, \tag{A 28}$$

$$\hat{I}_2 = \int_0^1 \mathrm{d}x \frac{(1-x^2)^2}{[1+cx^2]} = A_1 - \left(\frac{2c+1}{c}\right)A_2 + \frac{1}{3c}, \tag{A 29}$$

$$\begin{aligned}\hat{I}_3 &= \int_0^1 \mathrm{d}x \frac{x^4}{[1+cx^2]}\left[1+\frac{b^2[1+(a^2-1)x^2]}{[1+\mathrm{c}x^2]}\right] \\ &= \frac{1}{c}\left[\left(\frac{c+b^2(a^2-1)}{3c}\right) - \left(\frac{c(1-b^2)+b^2(a^2-1)}{c}\right)A_2 - b^2 A_3 - b^2(a^2-1)A_4\right],\end{aligned} \tag{A 30}$$

$$\begin{aligned}\hat{I}_4 &= b^2\int_0^1 \mathrm{d}x \frac{x^2(1-x^2)[1+(a^2-1)x^2]}{[1+cx^2]^2} \\ &= b^2\left\{A_3 - A_4 + \left(\frac{a^2-1}{c}\right)\left[\left(\frac{c+1}{c}\right)A_2 - \frac{1}{3c} + A_4 - A_3\right]\right\},\end{aligned} \tag{A 31}$$

where $A_1 - A_4$ are given by (A 7)–(A 10). It then follows that

$$\begin{gathered} I_1 = \tfrac{1}{4}[3\hat{I}_1 + \hat{I}_4], \quad I_2 = \hat{I}_1, \quad I_3 = \hat{I}_3, \\ I_4 = \hat{I}_2, \quad I_5 = \tfrac{1}{4}[\hat{I}_1 - \hat{I}_4], \quad \text{and} \quad I_6 = \tfrac{1}{4}[\hat{I}_1 + 3\hat{I}_4]. \end{gathered} \tag{A 32}$$

We note from (A 27) that λ is proportional to B and from (A 20) that B increases

rapidly as the lengthscales μ_h and μ_v are decreased. Thus, the nonlinear energy increases rapidly with decreasing Lagrangian lengthscale.

Appendix B. The calculation of $M_{33}(\boldsymbol{R}, \boldsymbol{m}, \tau)$

In this Appendix we obtain an exact expression for the function $M_{33}(\boldsymbol{R}, \boldsymbol{m}, \tau)$ which was defined in (3.10). The calculations outlined here are extremely tedious but the final result, while complicated, is tractable. The statistical calculations we will consider here are intricate and it is helpful to write the various expressions in terms of real independent dynamical variables instead of the complex p_j and q_j. Our calculations will also involve two different times separated by τ, and it is important to express the dynamical variables all at the same time and then use the weak interaction approximation to express the τ dependence explicitly. This has been done in (2.14) which can be used to rewrite the Lagrangian displacement in the compact form

$$s_{L\alpha}(\boldsymbol{r}, t+\tau) = \sum_{j=1}^{M} \sum_{m=1}^{2} \sum_{n=1}^{2} h_{jmn\alpha}(\boldsymbol{r}, \tau)\, u_{jmn}(t) = \sum_{\nu=1}^{4M} h_{\nu\alpha}(\boldsymbol{r}, \tau)\, u_\nu(t), \tag{B 1}$$

where the single sum over ν stands for the triple sum over j, m, and n,

$$u_{jmn}(t) = \delta_{n1}\, q_{jm}(t) + \delta_{n2}\, p_{jm}(t), \tag{B 2}$$

$$h_{jmn\alpha}(\boldsymbol{r}, \tau) = \left(\frac{2}{V\rho\Omega_j}\right)^{\frac{1}{2}} g_{jn\alpha}(\tau)\,[\delta_{m1} \cos(\boldsymbol{l}_j \cdot \boldsymbol{r}) - \delta_{m2} \sin(\boldsymbol{l}_j \cdot \boldsymbol{r})], \tag{B 3}$$

$$g_{j11}(\tau) = -\frac{l_{j3}}{l_j l_{jh}}\left[l_{j1} \cos(\Omega_j \tau) + \frac{f}{\Omega_j} l_{j2} \sin(\Omega_j \tau)\right], \tag{B 4}$$

$$g_{j12}(\tau) = -\frac{l_{j3}}{l_j l_{jh}}\left[l_{j2} \cos(\Omega_j \tau) - \frac{f}{\Omega_j} l_{j1} \sin(\Omega_j \tau)\right], \tag{B 5}$$

$$g_{j13}(\tau) = \frac{l_{jh}}{l_j} \cos(\Omega_j \tau), \tag{B 6}$$

$$g_{j21}(\tau) = \frac{l_{j3}}{l_j l_{jh}}\left[\frac{f}{\Omega_j} l_{j2} \cos(\Omega_j \tau) - l_{j1} \sin(\Omega_j \tau)\right], \tag{B 7}$$

$$g_{j22}(\tau) = -\frac{l_{j3}}{l_j l_{jh}}\left[\frac{f}{\Omega_j} l_{j1} \cos(\Omega_j \tau) + l_{j2} \sin(\Omega_j \tau)\right], \tag{B 8}$$

and

$$g_{j23}(\tau) = \frac{l_{jh}}{l_j} \sin(\Omega_j \tau). \tag{B 9}$$

By using (2.6) and (B 2) the free-field Hamiltonian can be written

$$H_0(s) = \sum_{\nu=1}^{4M} \tfrac{1}{2}\Omega_\nu u_\nu^2, \tag{B 10}$$

and by using (2.7) and (B 2) the phase-space density function can be written

$$g(u) = \sum_{\nu=1}^{4M} \left(\frac{\Omega_\nu}{2\pi\Lambda_\nu}\right)^{\frac{1}{2}} \exp\left\{-\frac{\Omega_\nu}{2\Lambda_\nu} u_\nu^2\right\}, \tag{B 11}$$

where we have suppressed explicit display of the time t.

The above expressions can now be used to compute $M_{33}(\boldsymbol{R}, \boldsymbol{m}, \tau)$. The expression given by (3.10) assumed spatial homogeneity and equated $\boldsymbol{m}$ to $\boldsymbol{m}'$. In order to demonstrate spatial homogeneity we require a more general expression which by using (A 14) can be written

$$M_{33}(\boldsymbol{R}, \boldsymbol{m}, \boldsymbol{m}', \tau) = E[\{s_{31} + (s_{31}\, s_{22} - s_{32}\, s_{21})\} \times \{s'_{31} + (s'_{31}\, s'_{22} - s'_{32}\, s'_{21})\} \exp\{-\mathrm{i}[\boldsymbol{m}\cdot\boldsymbol{s} - \boldsymbol{m}'\cdot\boldsymbol{s}']\}], \quad \text{(B 12)}$$

where we have suppressed display of the arguments $\boldsymbol{r}$ and t, the subscript L, and the prime on $\boldsymbol{s}$ and its components denote that its arguments are $\boldsymbol{r}'$ and t'. By using (B 1) the argument of the complex exponential in (B 12) can be written

$$[\boldsymbol{m}\cdot\boldsymbol{s} - \boldsymbol{m}'\cdot\boldsymbol{s}'] = \sum_{\nu=1}^{4M} Q_\nu u_\nu, \quad \text{(B 13)}$$

where

$$Q_\nu = \sum_{\alpha=1}^{3} [m_\alpha h_{\nu\alpha} - m'_\alpha h'_{\nu\alpha}]. \quad \text{(B 14)}$$

The evaluation of the expectation value in (B 12) will involve, apart from the complex exponential, products of displacements which are of quadratic, cubic, and quartic order. Thus, by using (B 1) in (B 12) it is easy to see that we will require expectation values of the form

$$\langle u_{\nu_1} \dots u_{\nu_n} \rangle = E\left[u_{\nu_1} \dots u_{\nu_n} \exp\left\{-\mathrm{i} \sum_{\nu=1}^{4M} Q_\nu u_\nu\right\}\right], \quad \text{(B 15)}$$

where $2 \leqslant n \leqslant 4$. It is then straightforward by using (B 11) and (B 15) to show that

$$\langle u_{\nu_1} \dots u_{\nu_n} \rangle = (i)^n \frac{\partial}{\partial Q_{\nu_1}} \dots \frac{\partial}{\partial Q_{\nu_n}} E(Q), \quad \text{(B 16)}$$

where

$$E(Q) = \exp\left\{-\frac{1}{2} \sum_{\nu=1}^{4M} \frac{\Lambda_\nu}{\Omega_\nu} Q_\nu^2\right\}. \quad \text{(B 17)}$$

By using (B 16) all of the terms in (B 12) can be evaluated exactly.

We shall illustrate the procedure by considering the term which is quadratic in the displacements. In order to evaluate this term we will require the expectation value $\langle u_{\nu_1} u_{\nu_2} \rangle$ which by using (B 16) and (B 17) is found to be

$$\langle u_{\nu_1} u_{\nu_2} \rangle = \left[\frac{\Lambda_{\nu_1}}{\Omega_{\nu_1}} \delta_{\nu_1 \nu_2} - \frac{\Lambda_{\nu_1} \Lambda_{\nu_2}}{\Omega_{\nu_1} \Omega_{\nu_2}} Q_{\nu_1} Q_{\nu_2}\right] E(Q). \quad \text{(B 18)}$$

Then by using (B 1), (B 3)–(B 9), and (B 18) it is tedious but straightforward to show that

$$\langle s_{31}\, s'_{31} \rangle = -\left[\frac{\partial^2 C_{\mathrm{Ls}33}(\boldsymbol{R}, \tau)}{\partial R_1^2} - \frac{\partial K_3(\boldsymbol{R}, \boldsymbol{m}, \tau)}{\partial R_1} \frac{\partial K_3(\boldsymbol{R}, \boldsymbol{m}', \tau)}{\partial R_1}\right] E(Q), \quad \text{(B 19)}$$

where the bracket $\langle\ \rangle$ denotes an expectation value of the form given by (B 15) and

$$K_\alpha(\boldsymbol{R}, \boldsymbol{m}, \tau) = \sum_{\beta=1}^{3} C_{\mathrm{Ls}\alpha\beta}(\boldsymbol{R}, \tau)\, m_\beta. \quad \text{(B 20)}$$

In obtaining (B 19) we have used

$$\sum_{\nu=1}^{4M} \frac{\Lambda_\nu}{\Omega_\nu} \frac{\partial h_{\nu\alpha}(\boldsymbol{r},t)}{\partial r_\gamma} \frac{\partial h_{\nu\beta}(\boldsymbol{r}',t')}{\partial r_\zeta} = -\frac{\partial^2 C_{\mathrm{Ls}\alpha\beta}(\boldsymbol{R},\tau)}{\partial R_\gamma \partial R_\zeta}, \tag{B 21}$$

$$\sum_{\nu=1}^{4M} \frac{\Lambda_\nu}{\Omega_\nu} \frac{\partial h_{\nu\alpha}(\boldsymbol{r},t)}{\partial r_\gamma} h_{\nu\beta}(\boldsymbol{r}',t') = \frac{\partial C_{\mathrm{Ls}\alpha\beta}(\boldsymbol{R},\tau)}{\partial R_\gamma}, \tag{B 22}$$

and

$$\frac{\partial C_{\mathrm{Ls}\alpha\beta}(0,\tau)}{\partial R_\gamma} = 0. \tag{B 23}$$

The argument of (B 17) can be evaluated by using (B 3)–(B 9) and (B 14) to obtain

$$\sum_{\nu=1}^{4M} \frac{\Lambda_\nu}{\Omega_\nu} Q_\nu^2 = \sum_{\alpha=1}^{3} \sum_{\beta=1}^{3} [(m_\alpha m_\beta + m'_\alpha m'_\beta) C_{\mathrm{Ls}\alpha\beta}(0,0) - (m_\alpha m'_\beta + m'_\alpha m_\beta) C_{\mathrm{Ls}\alpha\beta}(\boldsymbol{R},\tau)]. \tag{B 24}$$

We note that (B 24) and hence $E(Q)$ is spatially homogeneous. Therefore, (B 19) is also spatially homogeneous. While we have illustrated the procedure by considering the simplest term in (B 12), the calculation of all of the others, albeit more tedious, are entirely similar. It is found that all of the other terms are spatially homogeneous and hence (B 12) is spatially homogeneous. We have thus verified the homogeneity property used in obtaining (3.9) and may set $\boldsymbol{m} = \boldsymbol{m}'$ and suppress the display of $\boldsymbol{m}'$. By using the above procedure it can be shown that

$$M_{33}(\boldsymbol{R},\boldsymbol{m},\tau) = G_{33}(\boldsymbol{R},\boldsymbol{m},\tau) \exp\left\{ -\sum_{\alpha=1}^{3} \sum_{\beta=1}^{3} m_\alpha D_{\alpha\beta}(\boldsymbol{R},\tau) m_\beta \right\}, \tag{B 25}$$

and

$$D_{\alpha\beta}(\boldsymbol{R},\tau) = C_{\mathrm{Ls}\alpha\beta}(0,0) - C_{\mathrm{Ls}\alpha\beta}(\boldsymbol{R},\tau). \tag{B 26}$$

The expression for $G_{33}(\boldsymbol{R},\boldsymbol{m},\tau)$ can be written in terms of

$$C_{\alpha\beta\gamma\zeta} = \frac{\partial^2 C_{\mathrm{Ls}\alpha\beta}(\boldsymbol{R},\tau)}{\partial R_\gamma \partial R_\zeta}, \tag{B 27}$$

and

$$K_{\alpha\beta} = \frac{\partial K_\alpha(\boldsymbol{R},\tau)}{\partial R_\beta}, \tag{B 28}$$

such that

$$\begin{aligned} G_{33}(\boldsymbol{R},\boldsymbol{m},\tau) = \{ & -C_{3311} - K_{31}K_{31} - 2\mathrm{i}[C_{3311}K_{22} + C_{2312}K_{31} - C_{3312}K_{21} - C_{2311}K_{32} \\ & + K_{31}(K_{31}K_{22} - K_{32}K_{21})] + C_{3311}C_{2222} + C_{3322}C_{2211} - 2C_{3312}C_{2212} + 2C_{2312}C_{2312} \\ & - 2C_{2311}C_{2322} + C_{3311}K_{22}K_{22} + C_{3322}K_{21}K_{21} - 2C_{3312}K_{21}K_{22} + 2C_{2312}K_{22}K_{31} \\ & + 2C_{2312}K_{21}K_{32} - 2C_{2311}K_{22}K_{32} - 2C_{2322}K_{21}K_{31} + C_{2211}K_{32}K_{32} + C_{2222}K_{31}K_{31} \\ & - 2C_{2212}K_{31}K_{32} + K_{31}K_{31}K_{22}K_{22} + K_{32}K_{32}K_{21}K_{21} - 2K_{31}K_{22}K_{32}K_{21}\}. \end{aligned} \tag{B 29}$$

While the expression given by (B 29) is complicated and leads to subsequent tedious calculations, it is tractable and can be used to obtain exact expressions for the various Eulerian spectra.

Appendix C. The computation of $S_{\mathrm{Es}33}(\boldsymbol{k},\omega)$

As has been pointed out in §3, if at least one of the k_α is large, then the dominant contribution to the integral in (3.1) comes from values of both $\boldsymbol{R}$ and τ which are small. Because of the structure of the $C_{\mathrm{Ls}\alpha\beta}(\boldsymbol{R},\tau)$ the lowest-order correction terms, which are quadratic in $\boldsymbol{R}$ and τ, are additive. Since the function $G_{33}(\boldsymbol{R},\boldsymbol{k},\tau)$ involves derivatives with respect to the R_α we may write the approximation

$$S_{\mathrm{Es}33}(\boldsymbol{k},\omega) \approx \frac{1}{k_1^2}\int \mathrm{d}^3R \int \mathrm{d}\tau\, G_{33}(\boldsymbol{R},\boldsymbol{k},0)\exp\left\{-\sum_{\alpha=1}^{3}\sum_{\beta=1}^{3} k_\alpha D_{\alpha\beta}(\boldsymbol{R},0)\,k_\beta\right\} \times \exp\{-\mathrm{i}(\boldsymbol{k}\cdot\boldsymbol{R}-\omega\tau)-\tau^2(\eta_{\mathrm{h}}^2 k_{\mathrm{h}}^2+\eta_{\mathrm{v}}^2 k_3^2)\}, \quad \text{(C 1)}$$

where

$$\eta_{\mathrm{h}}^2 = \frac{E_0}{2(2\pi)^3\rho}\int \mathrm{d}^3l h(\boldsymbol{l})\frac{l_3^2}{l^2 l_{\mathrm{h}}^2}\left(l_1^2+\frac{f^2 l_2^2}{\Omega^2(\boldsymbol{l})}\right), \quad \text{(C 2)}$$

$$\eta_{\mathrm{v}}^2 = \frac{E_0}{2(2\pi)^3\rho}\int \mathrm{d}^3l h(\boldsymbol{l})\frac{l_{\mathrm{h}}^2}{l^2}, \quad \text{(C 3)}$$

and it is assumed that $h(\boldsymbol{l})$ is of the form given by (2.38). The τ integration may now be performed to obtain the result given in (3.19) and (3.20).

To evaluate (C 2) and (C 3) we use (2.5) and (2.38) to obtain

$$\eta_{\mathrm{h}}^2 = \frac{E_0}{8\pi^2\rho}\int_0^\infty \mathrm{d}x \int_0^\infty \mathrm{d}y \frac{yx^2}{x^2+y^2}\exp\{-\tfrac{1}{2}[\mu_{\mathrm{h}}^2 y^2+\mu_{\mathrm{v}}^2 x^2]\}\left[1+\frac{1}{b}\exp\left\{-\left(\frac{1-b^2}{2b^2}\right)\mu_{\mathrm{v}}^2 x^2\right\}\right], \quad \text{(C 4)}$$

and

$$\eta_{\mathrm{v}}^2 = \frac{E_0}{4\pi^2\rho}\int_0^\infty \mathrm{d}x \int_0^\infty \mathrm{d}y \frac{y^3}{x^2+y^2}\exp\{-\tfrac{1}{2}[\mu_{\mathrm{h}}^2 y^2+\mu_{\mathrm{v}}^2 x^2]\}, \quad \text{(C 5)}$$

where b is defined in (A 3). The above integrals reduce to standard forms which are readily evaluated to yield

$$\eta_{\mathrm{h}}^2 = \frac{\sqrt{2E_0}}{16(\pi^3)^{\frac{1}{2}}\rho\mu_{\mathrm{v}}^3}[L(a)+b^2 L(ab)], \quad \text{(C 6)}$$

$$\eta_{\mathrm{v}}^2 = \frac{\sqrt{2E_0}}{8(\pi^3)^{\frac{1}{2}}\rho\mu_{\mathrm{v}}^3}\left[\frac{1}{a^2}-L(a)\right], \quad \text{(C 7)}$$

where a is defined in (A 3) and

$$L(x) = \frac{1}{x^2-1}\left[1-\frac{1}{(x^2-1)^{\frac{1}{2}}}\tan^{-1}(x^2-1)^{\frac{1}{2}}\right]. \quad \text{(C 8)}$$

The approximate expression for $S_{\mathrm{Es}33}(\boldsymbol{k},\omega)$ given by (3.19) involves the wavenumber spectrum $\hat{S}_{\mathrm{Es}33}(\boldsymbol{k})$ defined by (3.20). We shall now obtain an approximate expression for $\hat{S}_{\mathrm{Es}33}(\boldsymbol{k})$ which is valid if any one of the k_α is large. It is clear from the length of the expression for $G_{33}(\boldsymbol{R},\boldsymbol{k},0)$ given by (B 29) that the following calculation is extremely detailed. What we shall do here is sketch out the salient steps and then simply state the final answer. We first consider the exponential factor in $M_{33}(\boldsymbol{R},\boldsymbol{k},0)$ and expand the various $D_{\alpha\beta}(\boldsymbol{R},0)$ in powers of the R_α. The resultant expression

contains cross-terms of the form $R_\alpha R_\beta$ and it is convenient to eliminate them by means of the transformation

$$w_1 = \frac{1}{k_h}(k_1 R_1 + k_2 R_2), \tag{C 9}$$

$$w_2 = \frac{1}{k_h}(k_1 R_2 - k_2 R_1), \tag{C 10}$$

and

$$w_3 = R_3 - \frac{8\bar{a}k_h k_3 w_1}{\bar{C}}, \tag{C 11}$$

where $\bar{a}$ and $\bar{C}$ are independent of $\boldsymbol{R}$ and will be defined in what follows. The expression for $\hat{S}_{Es33}(\boldsymbol{k})$ then takes the form

$$\hat{S}_{Es33}(\boldsymbol{k}) = \frac{1}{k_1^2}\int \mathrm{d}^3 w G_{33}(\boldsymbol{w}, \boldsymbol{k}) \exp\{-\mathrm{i}(k_3 w_3 + \bar{k} w_1) - (\bar{A} w_1^2 + \bar{B} w_2^2 + \bar{C} w_3^2)\}, \tag{C 12}$$

where

$$\bar{A} = (3\bar{a} + \bar{b}) k_h^2 + 4\bar{e}k_3^2 - \frac{64\bar{a}^2 k_h^2 k_3^2}{\bar{C}}, \tag{C 13}$$

$$\bar{B} = (\bar{a} + 3\bar{b}) k_h^2 + 4\bar{e}k_3^2, \tag{C 14}$$

$$\bar{C} = 4(\bar{c}k_h^2 + 2\bar{a}k_3^2), \tag{C 15}$$

$$\bar{k} = k_h\left(1 + \frac{8\bar{a}k_3^2}{\bar{C}}\right), \tag{C 16}$$

$$\bar{a} = \tfrac{1}{8}B\hat{I}_1, \tag{C 17}$$

$$\bar{b} = \tfrac{1}{8}B\hat{I}_4, \tag{C 18}$$

$$\bar{c} = \tfrac{1}{8}Ba^2\hat{I}_3, \tag{C 19}$$

$$\bar{e} = \tfrac{1}{8}\frac{B}{a^2}\hat{I}_2, \tag{C 20}$$

and the quantities a, B, and $\hat{I}_j$ were defined in Appendix B.

The three-dimensional integration over $\boldsymbol{w}$ can then be written as a product of three one-dimensional integrals of the form

$$\int_{-\infty}^{\infty} \mathrm{d}w\, w^n \exp\{-\alpha w^2 - \mathrm{i}\beta w\} = \frac{(-\mathrm{i})^n \pi^{\frac{1}{2}}}{2^n(\alpha^{n+1})^{\frac{1}{2}}} \exp\left(-\frac{\beta^2}{4\alpha}\right) H_n\left(\frac{\beta}{2\alpha^{\frac{1}{2}}}\right), \tag{C 21}$$

where $H_n(x)$ is a Hermite polynomial. The final result of the computation is

$$\hat{S}_{Es33}(\boldsymbol{k}) = \frac{1}{k_1^2}\left(\frac{\pi^3}{\bar{A}\bar{B}\bar{C}}\right)^{\frac{1}{2}} \exp\left\{-\frac{1}{4}\left(\frac{\bar{k}^2}{\bar{A}} + \frac{k_3^2}{\bar{C}}\right)\right\} \tilde{S}(\hat{\boldsymbol{k}}), \tag{C 22}$$

where $\tilde{S}(\boldsymbol{k})$ depends upon the unit vector $\hat{\boldsymbol{k}}$ but not upon the magnitude k. The full expression for $\tilde{S}(\boldsymbol{k})$ is extremely complicated but can be written as a sum of terms such that

$$\tilde{S}(\hat{\boldsymbol{k}}) = \tilde{S}_1(\hat{\boldsymbol{k}}) - 16\tilde{S}_2(\hat{\boldsymbol{k}}) + 16\tilde{S}_3(\hat{\boldsymbol{k}}) - 32\tilde{S}_4(\hat{\boldsymbol{k}}) + \tilde{S}_5(\hat{\boldsymbol{k}}) - 8\tilde{S}_6(\hat{\boldsymbol{k}}) + 16\tilde{S}_7(\hat{\boldsymbol{k}}), \tag{C 23}$$

$$\tilde{S}_1(\hat{\boldsymbol{k}}) = 8\bar{e}, \tag{C 24}$$

$$\tilde{S}_2(\hat{\boldsymbol{k}}) = \frac{\bar{a}^2 k_1^2}{\bar{C}}\left(2-\frac{k_3^2}{\bar{C}}\right) - \frac{2\bar{a}k_1^2 k_3^2 \bar{k}\bar{D}}{k_\mathrm{h}\bar{A}\bar{C}} + \frac{2\bar{e}^2 k_2^2 k_3^2}{k_\mathrm{h}^2 \bar{B}} + \frac{k_1^2 k_3^2 \bar{D}^2}{k_\mathrm{h}^2 \bar{A}}\left(2-\frac{\bar{k}^2}{\bar{A}}\right), \tag{C 25}$$

$$\tilde{S}_3(\hat{\boldsymbol{k}}) = \frac{4\bar{a}\bar{e}k_3^2}{\bar{C}} + \frac{\bar{e}\bar{k}}{k_\mathrm{h}\bar{A}}\left[k_1^2(\bar{b}-\bar{a}) - k_2^2(3\bar{a}+\bar{b}) + \frac{32\bar{a}^2 k_\mathrm{h}^2 k_3^2}{\bar{C}}\right], \tag{C 26}$$

$$\begin{aligned}\tilde{S}_4(\boldsymbol{k}) = {} & \frac{4\bar{a}^3 k_1^2 k_3^2}{\bar{C}^2}\left(6-\frac{k_3^2}{\bar{C}}\right) + \frac{\bar{a}^2 k_1^2 \bar{k}}{k_\mathrm{h}\bar{A}\bar{C}}\left(2-\frac{k_3^2}{\bar{C}}\right)\left[(\bar{b}-\bar{a})\,k_\mathrm{h}^2 + 4\left(\frac{16\bar{a}^2 k_\mathrm{h}^2}{\bar{C}} - \bar{e}\right)k_3^2\right] \\ & + \frac{2\bar{a}\bar{e}(\bar{b}-\bar{a})\,k_1^2 k_3^2}{\bar{B}\bar{C}} + \frac{\bar{a}k_1^2 k_3^2 \bar{D}}{\bar{A}\bar{C}}\left(2-\frac{\bar{k}^2}{\bar{A}}\right)\left[(\bar{b}-\bar{a}) + \frac{32\bar{a}^2 k_3^2}{\bar{C}}\right] + \frac{2\bar{a}\bar{e}k_2^2 k_3^2}{k_\mathrm{h}^2 \bar{B}\bar{C}}\left[4\bar{e}k_3^2 - (\bar{a}+3\bar{b})\,k_\mathrm{h}^2\right] \\ & + \frac{4\bar{e}k_2^2 k_3^2 \bar{k}}{k_\mathrm{h}\bar{A}\bar{B}}\left[\frac{16\bar{a}^2\bar{e}k_3^2}{\bar{C}} + \bar{e}(\bar{b}-\bar{a}) - \frac{4\bar{a}^2 k_\mathrm{h}^2(\bar{a}+3\bar{b})}{\bar{C}}\right] + \frac{4\bar{a}^2 k_1^2 k_3^2 \bar{k}\bar{D}}{k_\mathrm{h}\bar{A}\bar{C}}\left(2-\frac{k_3^2}{\bar{C}}\right) \\ & + \frac{\bar{a}k_1^2 k_3^2 \bar{D}}{k_\mathrm{h}^2 \bar{A}\bar{C}}\left(2-\frac{\bar{k}^2}{\bar{A}}\right)\left[(\bar{b}-\bar{a})\,k_\mathrm{h}^2 + 4\left(\frac{16\bar{a}^2 k_\mathrm{h}^2}{\bar{C}} - \bar{e}\right)k_3^2\right] + \frac{2\bar{e}(\bar{b}-\bar{a})\,k_1^2 k_3^2 \bar{k}\bar{D}}{k_\mathrm{h}\bar{A}\bar{B}} \\ & + \frac{k_1^2 k_3^2 \bar{k}\bar{D}^2}{k_\mathrm{h}\bar{A}^2}\left(6-\frac{\bar{k}^2}{\bar{A}}\right)\left[(\bar{b}-\bar{a}) + \frac{32\bar{a}^2 k_3^2}{\bar{C}}\right],\end{aligned} \tag{C 27}$$

$$S_5(\hat{\boldsymbol{k}}) = 64\bar{e}(\bar{a}+\bar{b}), \tag{C 28}$$

$$\begin{aligned}\tilde{S}_6(\hat{\boldsymbol{k}}) = {} & \frac{4\bar{a}^2}{\bar{C}}\left(2-\frac{k_3^2}{\bar{C}}\right)[4\bar{e}k_3^2 + (\bar{a}+3\bar{b})\,k_2^2 + (3\bar{a}+\bar{b})\,k_1^2] \\ & - \frac{16\bar{a}k_3^2 \bar{k}}{k_\mathrm{h}\bar{A}\bar{C}}\left[\frac{16\bar{e}\bar{a}^2 k_\mathrm{h}^2 k_3^2}{\bar{C}} - k_1^2\left\langle 2\bar{a}\bar{e} - \frac{4\bar{a}^2 k_\mathrm{h}^2}{\bar{C}}(3\bar{a}+\bar{b})\right\rangle\right. \\ & \left. - k_2^2\left\langle 2\bar{e}(\bar{a}+\bar{b}) - \frac{4\bar{a}^2 k_\mathrm{h}^2}{\bar{C}}(\bar{a}+3\bar{b})\right\rangle\right] \\ & + \frac{2\bar{e}}{k_\mathrm{h}^2 \bar{B}}[4\bar{e}k_3^2\langle(\bar{a}+3\bar{b})\,k_1^2 + (3\bar{a}+\bar{b})\,k_2^2\rangle \\ & + (\bar{a}-\bar{b})^2 k_1^4 + (\bar{a}+3\bar{b})^2 k_2^4 + 2k_1^2 k_2^2(\bar{a}^2 + 2\bar{a}\bar{b} + 5\bar{b}^2)] \\ & + \frac{1}{k_\mathrm{h}^2 \bar{A}}\left(2-\frac{\bar{k}^2}{\bar{A}}\right)\left[4k_3^2 \bar{D}^2\langle(3\bar{a}+\bar{b})\,k_1^2 + (\bar{a}+3\bar{b})\,k_2^2\rangle\right. \\ & + \bar{e}(\bar{a}-\bar{b})^2 k_1^4 + \bar{e}(3\bar{a}+\bar{b})^2 k_2^4 + 2\bar{e}k_1^2 k_2^2(5\bar{a}^2 + 2\bar{a}\bar{b} + \bar{b}^2) \\ & \left. - \frac{64\bar{a}^2\bar{e}k_\mathrm{h}^2 k_3^2}{\bar{C}}\left((\bar{a}-\bar{b})\,k_1^2 + (3\bar{a}+\bar{b})\,k_2^2 - \frac{16\bar{a}^2 k_\mathrm{h}^2 k_3^2}{\bar{C}}\right)\right],\end{aligned} \tag{C 29}$$

$$\begin{aligned}\tilde{S}_7(\hat{\boldsymbol{k}}) = {} & \frac{16\bar{a}^4 k_1^2 k_3^2}{\bar{C}^2}\left(12 - \frac{12k_3^2}{\bar{C}} + \frac{k_3^4}{\bar{C}^2}\right) + \frac{16\bar{a}^2\bar{e}k_1^2 k_3^2(\bar{b}-\bar{a})}{\bar{B}\bar{C}}\left(2-\frac{k_3^2}{\bar{C}}\right) \\ & - \frac{8\bar{a}^3 k_1^2 k_3^2 \bar{k}}{k_\mathrm{h}\bar{A}\bar{C}^2}\left(6-\frac{k_3^2}{\bar{C}}\right)\left[(\bar{b}-\bar{a})\,k_\mathrm{h}^2 + 4k_3^2\left(\frac{16\bar{a}^2 k_\mathrm{h}^2}{\bar{C}} - \bar{e}\right)\right] \\ & + \left(2-\frac{k_3^2}{\bar{C}}\right)\left[\frac{8\bar{a}^2 k_1^2 k_3^2 \bar{D}}{\bar{A}\bar{C}}\left(2-\frac{\bar{k}^2}{\bar{A}}\right)\left((\bar{b}-\bar{a}) + \frac{32\bar{a}^2 k_3^2}{\bar{C}}\right) + \frac{2\bar{a}^2 k_2^2}{k_\mathrm{h}^2 \bar{B}\bar{C}}(4\bar{e}k_3^2 - k_\mathrm{h}^2(\bar{a}+3\bar{b}))^2\right]\end{aligned}$$

$$-\frac{8\bar{a}k_2^2k_3^2\bar{k}}{k_h\bar{A}\bar{B}\bar{C}}\left[\frac{16\bar{e}\bar{a}^2k_3^2}{\bar{C}}+\bar{e}(\bar{b}-\bar{a})-\frac{4\bar{a}^2k_h^2(\bar{a}+3\bar{b})}{\bar{C}}\right][4\bar{c}k_3^2-k_h^2(\bar{a}+3\bar{b})]$$

$$+\frac{\bar{a}^2k_1^2}{k_h^2\bar{A}\bar{C}}\left(2-\frac{\bar{k}^2}{\bar{A}}\right)\left(2-\frac{k_3^2}{\bar{C}}\right)\left[(\bar{b}-\bar{a})\,k_h^2+4k_3^2\left(\frac{16\bar{a}^2k_h^2}{\bar{C}}-\bar{e}\right)\right]^2+\frac{12\bar{e}k_1^2\,k_3^2(\bar{b}-\bar{a})^2}{\bar{B}^2}$$

$$-\frac{4\bar{a}\bar{e}(\bar{b}-\bar{a})\,k_1^2\,k_3^2\,\bar{k}}{k_h\bar{A}\bar{B}\bar{C}}\left[(\bar{b}-\bar{a})\,k_h^2+4k_3^2\left(\frac{16\bar{a}^2k_h^2}{\bar{C}}-\bar{e}\right)\right]$$

$$-\frac{2\bar{a}\bar{D}k_1^2\,k_3^2\,\bar{k}}{k_h\bar{A}^2\bar{C}}\left(6-\frac{\bar{k}^2}{\bar{A}}\right)\left[(\bar{b}-\bar{a})\,k_h^2+4k_3^2\left(\frac{16\bar{a}^2k_h^2}{\bar{C}}-\bar{e}\right)\right]\left[(\bar{b}-\bar{a})+\frac{32\bar{a}^2k_3^2}{\bar{C}}\right]$$

$$+\frac{4\bar{e}\bar{D}(\bar{b}-\bar{a})\,k_1^2\,k_3^2}{\bar{A}\bar{B}}\left(2-\frac{\bar{k}^2}{\bar{A}}\right)\left[(\bar{b}-\bar{a})+\frac{32\bar{a}^2k_3^2}{\bar{C}}\right]$$

$$+\frac{\bar{D}^2k_1^2\,k_3^2}{\bar{A}^2}\left(12-12\frac{\bar{k}^2}{\bar{A}}+\frac{\bar{k}^4}{\bar{A}^2}\right)\left[(\bar{b}-\bar{a})+\frac{32\bar{a}^2k_3^2}{\bar{C}}\right]^2$$

$$+\frac{8k_2^2\,k_3^2}{\bar{A}\bar{B}}\left(2-\frac{\bar{k}^2}{\bar{A}}\right)\left[\frac{16\bar{e}\bar{a}^2k_3^2}{\bar{C}}+\bar{e}(\bar{b}-\bar{a})-\frac{4\bar{a}^2k_h^2}{\bar{C}}(\bar{a}+3\bar{b})\right]^2, \tag{C 30}$$

with

$$\bar{D}=\frac{8\bar{a}^2k_h^2}{\bar{C}}-\bar{e}. \tag{C 31}$$

By setting $\boldsymbol{k}=k\hat{\boldsymbol{k}}$ the form given by (3.21) is obtained.

The expression for $\mathrm{HTS}_{\mathrm{Es33}}(\kappa)$ is obtained by setting $k_1=\kappa$ and integrating (C 22) over k_2 and k_3. To simplify the calculation we make use of the fact that, for the values of the parameters used in this paper, B is of order unity, $a\gg 1$, $b\ll 1$, and ab is of order unity. Hence, $\bar{a}$ and $\bar{b}$ are of order unity while $\bar{c}\gg 1$ and $\bar{e}\ll 1$. Then $\bar{A}\approx k_h^2(3\bar{a}+\bar{b})$, $\bar{B}\approx k_h^2(\bar{a}+3\bar{b})$, $\bar{C}\approx 4\bar{c}k_h^2$, and $\bar{k}\approx k_h$. If we retain only the dominant terms in $\hat{S}_{\mathrm{Es33}}(\boldsymbol{k})$ and change the k_2 and k_3 to $k_2=\kappa\xi_2$ and $k_3=\kappa\xi_3$, then we find that the only ξ_3 dependence occurs in the exponential term $\exp\{-\xi_3^2/16\bar{c}(1+\xi_2^2)\}$ which permits the ξ_3 integration to be performed. The remaining ξ_2 integrations are then of a standard form and easily obtained. The result of the calculation is given by (3.26) where the constant W is given by

$$W=\frac{2\pi K}{((3\bar{a}+\bar{b})(3\bar{b}+\bar{a}))^{\frac{1}{2}}}\exp\left\{-\frac{1}{4(3\bar{a}+\bar{b})}\right\}, \tag{C 32}$$

and

$$K=\left[2\bar{e}-\frac{\bar{a}^2}{\bar{c}}-\frac{8\bar{a}\bar{e}}{3\bar{a}+\bar{b}}-\frac{2\bar{a}^2(\bar{b}-\bar{a})}{\bar{c}(3\bar{a}+\bar{b})}+\frac{2\bar{e}(\bar{b}^2+2\bar{a}\bar{b}+5\bar{a}^2)}{(3\bar{a}+\bar{b})^2}-\frac{\bar{a}^2(\bar{b}-\bar{a})^2}{\bar{c}(3\bar{a}+\bar{b})^2}\right]$$

$$+8\left[\frac{4(\bar{b}+\bar{a})(2\bar{c}\bar{e}-\bar{a}^2)}{\bar{c}}-\frac{2\bar{e}(\bar{b}^2+2\bar{a}\bar{b}+5\bar{a}^2)}{(3\bar{a}+\bar{b})}-\frac{2\bar{e}(\bar{a}^2+2\bar{a}\bar{b}+5\bar{b}^2)}{(3\bar{b}+\bar{a})}\right.$$

$$\left.+\frac{\bar{a}^2(\bar{a}+3\bar{b})}{\bar{c}}+\frac{\bar{a}^2(\bar{a}-\bar{b})^2}{\bar{c}(3\bar{a}+\bar{b})}\right]. \tag{C 33}$$

Similarly an expression for $\mathrm{VTS}_{\mathrm{Es33}}(\iota)$ can be obtained by setting $k_3=\iota$ and integrating (C 22) over k_1 and k_2. By making use of the approximations used in evaluating $\mathrm{HTS}_{\mathrm{Es33}}(\kappa)$, namely $\bar{a}$ and $\bar{b}$ are of order unity, $\bar{c}\gg 1$, $\bar{e}\ll 1$, $k_1=\iota\xi_1$, and

$k_2 = \iota\xi_2$, the resulting integrals are easily evaluated. The result is given by (3.29) with the constant $\overline{W}$ given by

$$\overline{W} = \frac{3^2 2^{11} \pi \bar{c}^2 \bar{e} (\bar{a}-\bar{b})^2}{((\bar{a}+3\bar{b})^5 (3\bar{a}+\bar{b}))^{\frac{1}{2}}} \exp\left\{\frac{-1}{4(3\bar{a}+\bar{b})}\right\}. \tag{C 34}$$

REFERENCES

ABARBANEL, H. D. I. & ROUHI, A. 1987 Phase space density representation of inviscid fluid dynamics. *Phys. Fluids* **30**, 2952–2964.

ALLEN, K. R. & JOSEPH, R. I. 1988 The relation between Lagrangian and Eulerian spectra: a connection between large-scale waves and small-scale turbulence. In *Small-Scale Turbulence and Mixing in the Ocean* (ed. J. C. J. Nihoul & B. M. Jamart), pp. 303–318. Elsevier.

CAIRNS, J. L. & WILLIAMS, G. O. 1976 Internal wave observations from a midwater float, 2. *J. Geophys. Res.* **81**, 1943–1950.

FLATTÉ, S. M., HENYEY, F. S. & WRIGHT, J. A. 1985 Eikonal calculations of short wavelength internal-wave spectra. *J. Geophys. Res.* **90** (c4), 7265–7272.

FOX, R. F. 1978 Gaussian stochastic processes in physics. *Phys. Rep.* **48**, 179–283.

GARRETT, C. J. R. & MUNK, W. H. 1972 Space–time scales of internal waves. *Geophys. Fluid Dyn.* **3**, 225–264.

GARRETT, C. J. R. & MUNK, W. H. 1975 Space–time scales of internal waves: a progress report. *J. Geophys. Res.* **80**, 291–297.

GREEN, M. S. 1954 Markoff random processes and the statistical mechanics of time-dependent processes. II. Irreversible processes in fluids. *J. Chem. Phys.* **22**, 398–413.

GREGG, M. C. 1977 A comparison of finestructure spectra from the main thermocline. *J. Phys. Oceanogr.* **7**, 33–40.

HARDY, R. J. 1963 Energy-flux operator for a lattice. *Phys. Rev.* **132**, 168–177.

HASSELMANN, K. 1966 Feynman diagrams and interaction rules of wave–wave scattering processes. *Rev. Geophys. Space Phys.* **4**, 1–32.

HENYEY, F. S. 1983 Hamiltonian description of stratified fluid dynamics. *Phys. Fluids* **26**, 40–47.

HENYEY, F. S. & POMPHREY, N. 1983 Eikonal description of internal wave interactions: A non-diffusive picture of induced diffusion. *Dyn. Atmos. Oceans* **7**, 189–219.

HOLLOWAY, G. 1980 Oceanic internal waves are not weak waves. *J. Phys. Oceanogr.* **10**, 906–914.

HOLLOWAY, G. 1981 Theoretical approaches to interactions among internal waves, turbulence, and finestructure. In *AIP Conference Proceedings no. 76* (ed. B. J. West), pp. 47–77.

HOLLOWAY, G. 1982 On interaction time scales of oceanic internal waves. *J. Phys. Oceanogr.* **12**, 293–296.

HOLLOWAY, G. 1986 Eddies, waves, circulation, and mixing: statistical geofluid mechanics. *Ann. Rev. Fluid Mech.* **18**, 91–147.

KAMPEN, N. G. VAN 1976 Stochastic differential equations. *Phys. Rep.* **24c**, 171–228.

KATZ, E. J. 1975 Tow spectra from MODE. *J. Geophys. Res.* **80**, 1163–1167.

LONGUET-HIGGINS, M. S. 1986 Eulerian and Lagrangian aspects of surface waves. *J. Fluid Mech.* **173**, 683–707.

MCCOMAS, C. H. & MÜLLER, P. 1981 The dynamic balance of internal waves. *J. Phys. Oceanogr.* **11**, 970–986.

MORI, H. 1965 Transport, collective motion, and Brownian motion. *Prog. Theor. Phys.* **33**, 423–455.

MORI, H., OPPENHEIM, I. & ROSS, J. 1962 Some topics in quantum statistics. The Wigner function and transport theory. In *Studies in Statistical Mechanics* (ed. J. DeBoer & G. E. Uhlenbeck), Vol. I, § c6, pp. 271–298. Interscience.

PHILLIPS, O. M. 1969 *The Dynamics of the Upper Ocean*. Cambridge University Press.

PINKEL, R. 1981 Observations of the near-surface internal wavefield. *J. Phys. Oceanogr.* **11**, 1248–1257.

PINKEL, R. 1984 Doppler sonar observations of internal waves: the wavenumber-frequency spectrum. *J. Phys. Oceanogr.* **14**, 1249–1270.

POMPHREY, N. 1981 Review of some calculations of energy transport in a Garrett–Munk ocean. In *AIP Conference Proceedings no. 76* (ed. B. J. West), pp. 113–128.

POMPHREY, N., MEISS, J. D. & WATSON, K. M. 1980 Description of nonlinear internal wave interactions using Langevin methods. *J. Geophys. Res.* **85** (c2), 1085–1094.

PRIGOGINE, I. 1962 *Non-Equilibrium Statistical Mechanics.* Interscience.

PRIGOGINE, I. & HENIN, F. 1957 On the general perturbational treatment of irreversible processes. *Physica* **23**, 585–596.

PRIGOGINE, I. & HENIN, F. 1960 On the general theory of the approach to equilibrium. I. Interacting normal modes. *J. Math. Phys.* **1**, 349–371.

SELIGER, R. L. & WHITHAM, G. B. 1968 Variational principles in continuum mechanics. *Proc. R. Soc. Lond.* A **305**, 1–25.

TAYLOR, G. I. 1921 Diffusion by continuous movements. *Proc. Lond. Math. Soc.* **20**, 196–212.

TOLSTOY, I. 1963 The theory of waves in stratified fluids including the effects of gravity and rotation. *Rev. Mod. Phys.* **35**, 207–230.

WEST, B. J. 1982 Resonant-test-field model of fluctuating nonlinear waves. *Phys. Rev.* A **25**, 1683–1691.